



This is a repository copy of *Remote-sensing-based analysis of the 1996 surge of Northern Inylchek Glacier, central Tien Shan, Kyrgyzstan.*

White Rose Research Online URL for this paper:
<http://eprints.whiterose.ac.uk/104037/>

Version: Accepted Version

Article:

Häusler, H., Ng, F. orcid.org/0000-0001-6352-0351, Kopecny, A. et al. (1 more author) (2016) Remote-sensing-based analysis of the 1996 surge of Northern Inylchek Glacier, central Tien Shan, Kyrgyzstan. *Geomorphology*, 273. pp. 292-307. ISSN 0169-555X

<https://doi.org/10.1016/j.geomorph.2016.08.021>

This manuscript version is made available under the CC-BY-NC-ND 4.0 license
<http://creativecommons.org/licenses/by-nc-nd/4.0/>

Reuse

This article is distributed under the terms of the Creative Commons Attribution-NonCommercial-NoDerivs (CC BY-NC-ND) licence. This licence only allows you to download this work and share it with others as long as you credit the authors, but you can't change the article in any way or use it commercially. More information and the full terms of the licence here: <https://creativecommons.org/licenses/>

Takedown

If you consider content in White Rose Research Online to be in breach of UK law, please notify us by emailing eprints@whiterose.ac.uk including the URL of the record and the reason for the withdrawal request.



eprints@whiterose.ac.uk
<https://eprints.whiterose.ac.uk/>

Accepted Manuscript

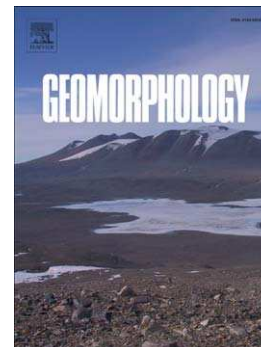
Remote-sensing-based analysis of the 1996 surge of Northern Inylchek Glacier, central Tien Shan, Kyrgyzstan

Hermann Häusler, Felix Ng, Alexander Kopecny, Diethard Leber

PII: S0169-555X(16)30725-5
DOI: doi: [10.1016/j.geomorph.2016.08.021](https://doi.org/10.1016/j.geomorph.2016.08.021)
Reference: GEOMOR 5735

To appear in: *Geomorphology*

Received date: 26 January 2016
Revised date: 11 August 2016
Accepted date: 14 August 2016



Please cite this article as: Häusler, Hermann, Ng, Felix, Kopecny, Alexander, Leber, Diethard, Remote-sensing-based analysis of the 1996 surge of Northern Inylchek Glacier, central Tien Shan, Kyrgyzstan, *Geomorphology* (2016), doi: [10.1016/j.geomorph.2016.08.021](https://doi.org/10.1016/j.geomorph.2016.08.021)

This is a PDF file of an unedited manuscript that has been accepted for publication. As a service to our customers we are providing this early version of the manuscript. The manuscript will undergo copyediting, typesetting, and review of the resulting proof before it is published in its final form. Please note that during the production process errors may be discovered which could affect the content, and all legal disclaimers that apply to the journal pertain.

Remote-sensing-based analysis of the 1996 surge of Northern Inylchek Glacier, central Tien Shan, Kyrgyzstan

Hermann Häusler ^{a*} • Felix Ng ^b • Alexander Kopecny ^a • Diethard Leber ^a

^a Department of Environmental Geosciences, University of Vienna, Vienna, Austria

^b Department of Geography, University of Sheffield, Sheffield S10 2TN, UK

* Corresponding author: hermann.haeusler@univie.ac.at (H. Häusler)

Abstract

The evolution of Northern Inylchek Glacier and its proglacial lake - Upper Lake Merzbacher - during its 1996 surge and the surrounding decades is analyzed with remote sensing imagery. Overall retreat of the glacier from 1943 to 1996 enlarged the lake to 4 km long and ≈ 100 m deep. The surge in 1996 initiated between 12 September and 7 October and advanced the glacier by 3.7 km to override most of Upper Lake Merzbacher. The surge phase probably ended in December 1996 and involved mean flow velocities across the lower trunk of the glacier that reached 50 m d^{-1} over a 32-day period. Water displaced by the surge from Upper Lake Merzbacher, totalling $1.5 \times 10^8 \text{ m}^3$ in volume, accelerated filling of Lower Lake Merzbacher downvalley and helped trigger this marginal ice-dammed lake to outburst in a jökulhlaup around late November/early December. The characteristics and duration of the surge render it as similar to temperate glacier surges elsewhere. It may have been facilitated by low basal friction caused by water-saturated sediments in the upper lake bed. Furthermore, bathymetric measurements show that the surge evacuated much sediment into the upper lake, causing its depth to reduce from 20-30 m in 1996 to 8 m by 2005 and 2 m by 2011; the corresponding deposition rates imply glacier-catchment specific mean sediment yields of 1.4 to $3.4 \times 10^3 \text{ Mg km}^{-2} \text{ a}^{-1}$ in the years after the surge. Our study documents novel interactions within a cascade system of glaciers and lakes that exhibits surging and outburst-flood behavior.

Keywords Glacier surge, remote sensing, Lower Lake Merzbacher, Upper Lake Merzbacher, bathymetry, glacier lake outburst flood

1. Introduction

Surging describes an abrupt speedup of a glacier's flow over a period of months or years, which causes its snout to advance (Meier and Post, 1969; Harrison et al., 2014). Some surging glaciers switch repeatedly between this active surge phase, when ice transfers rapidly from the glacier's accumulation area toward its snout, and a longer quiescent phase - typically lasting decades - when flow speeds remain normal. Consequently, surges are often regarded today as a cyclical instability caused by internal switches in the basal conditions of the glacier, not exclusively as singular events triggered by external forcing (Benn and Evans, 2010, p. 187; Cuffey and Paterson, 2010). Sizeable populations of surging glaciers have been found in Alaska and Arctic Canada (Copland et al., 2003), Svalbard and East Greenland (Jiskoot et al., 2000), Iceland (Björnsson et al., 2003), the Karakoram (Gardner, 1990; Barrand and Murray, 2006; Mayer et al., 2011; Quincey et al., 2011; Hewitt, 2014), northwestern Himalaya (Philip and Sah, 2004) and the Pamir and Caucasus (Osipova et al., 1998; Kotlyakov et al., 2008, 2010; Evans et al., 2009).

Monitoring the long-term behaviour of surge-type glaciers and detailed study of individual surges is essential for improving our knowledge of the physical mechanisms behind surging (e.g., Kamb et al., 1985; Clarke, 1987; Raymond, 1987; Fowler et al., 2001; Harrison and Post, 2003; Frappé and Clarke, 2007), which has derived from a small subset of surges yielding relatively comprehensive observations. Regarding ice flow dynamics during a surge, two distinct kinds of behavior have been recognised: Alaskan and Svalbard. Alaskan-type surges have sudden onset, high maximum ice-flow velocities (of the order of 50 m d^{-1}) and sudden termination that may be accompanied by large discharges of water from the glacier. Typified by the 1982-83 surge of Variegated Glacier in Alaska (Kamb et al., 1985; Raymond, 1987), this kind of surge occurs on temperate-

based glaciers and is synonymous with what Hewitt (2014) terms the classic surge of Karakoram glaciers. In contrast, Svalbard-type surges have slow initiation that often involves the passage of a surge bulge/front downglacier, and a gradual rise to maximum flow velocities that are typically lower ($\sim 10 \text{ m d}^{-1}$); their active phase also tends to last longer (many years; e.g., Murray et al., 1998). Their occurrence is associated with glaciers with a polythermal base.

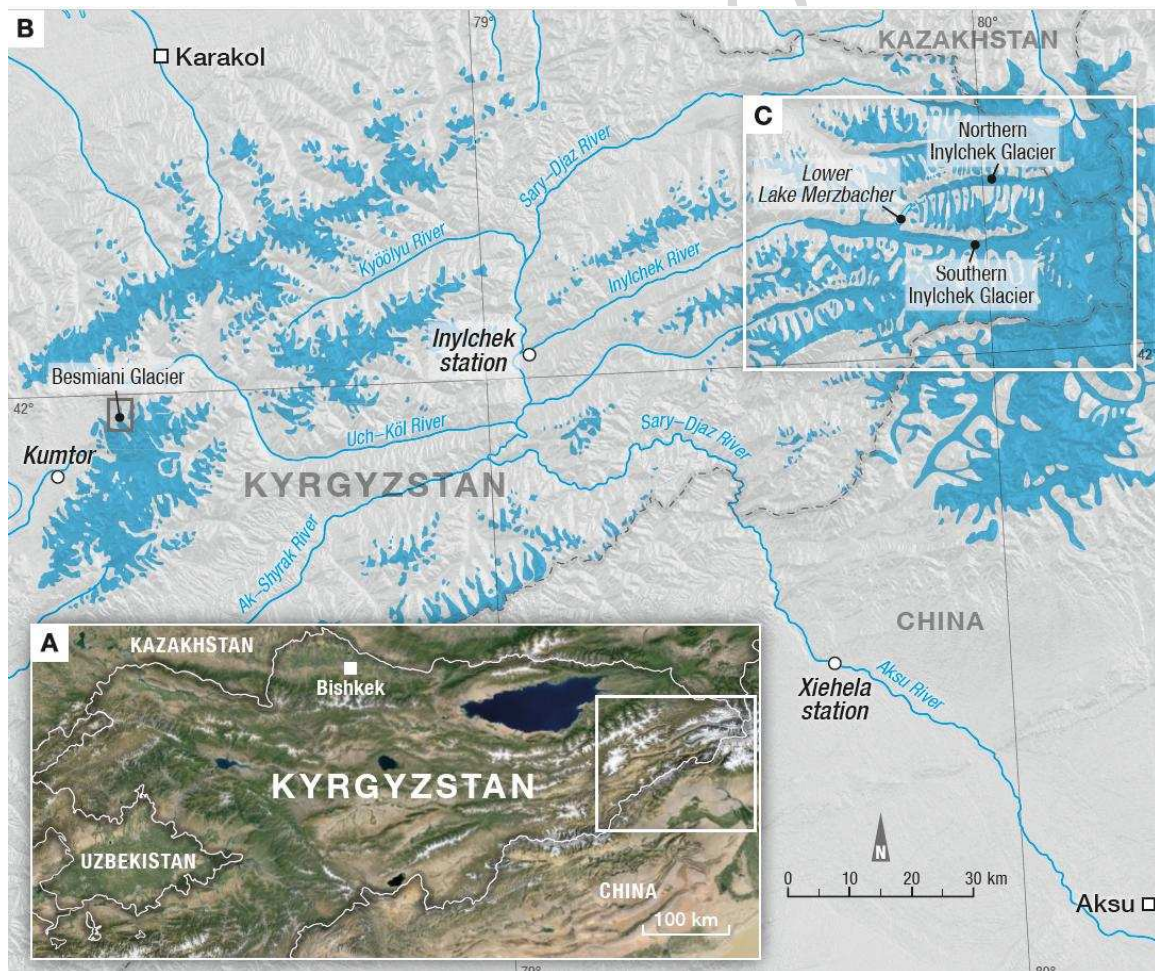


Fig. 1: Part of the Tien Shan in eastern Kyrgyzstan and neighbouring China (A). Context map; small box locates area of panel B. (B) Catchment of Sary-Djaz River, key hydrological stations, and several surging glaciers described in the text. White box outlines the Inylchek glacier system, expanded in Figure 2A.

In this paper, we use remote sensing imagery to study the dynamical and morphological evolution of Northern Inylchek Glacier, Kyrgyzstan, during its 1996 surge and the surrounding decades. We focus on changes in the glacier's lower trunk and snout position, and also examine the hydrological and sedimentological impacts of the surge.

The goal is to provide a first detailed analysis of a surge-type glacier in the central Tien Shan. Although the literature has reported glacier surges in Central Asia during the last century (Atlas of the Kyrgyz Republic, 1987), the few available investigations to date give a fragmented picture of surges across the region, making it difficult to discern a common pattern in their characteristics or underlying climatic, glaciological, or geologic controls. Besides the surge analysed in this paper, the only other documented surges within the Sary-Djaz River and Aksu River catchments of the Tien Shan (Fig. 1) are those of Mushketov Glacier in 1956-1957 (Kotlyakov et al., 2010), Kaindy Glacier in 1943-1960 (Atlas of the Kyrgyz Republic, 1987; Kotlyakov et al., 2010), and Besmiani Glacier (date unknown; Atlas of the Kyrgyz Republic, 1987); see Figs. 1 and 2A. In these catchments, remote sensing studies at decadal time resolution (Osmonov et al., 2013; Pieczonka et al., 2013; Pieczonka and Bolch, 2015) have also detected anomalous advances of Samoilowitsch Glacier (also called Glacier No. 377) and Qingbingtan Glacier No. 74 between 1990-2010 and 1999-2009, respectively, and attributed these changes to surge activity. But none of the surge sequences of the glaciers mentioned here have been explored in detail.

Northern Inylchek Glacier and its neighbour Southern Inylchek Glacier comprise the largest compound glacier system in the central Tien Shan (Figs. 1 and 2). Monitoring the fluctuation of glaciers in this region is important as they are a key contributor of water to rivers feeding settlements around the Tarim Basin (e.g., Aizen and Aizen, 1997). The Inylchek system is relevant from the glacial hazards perspective as well. As described below, Northern Inylchek Glacier terminates in a proglacial lake, and downvalley lies an ice-dammed lake (impounded by Southern Inylchek Glacier) that has repeatedly outburst to deliver glacier outburst floods or jökulhlaups. This unique arrangement means that advance and retreat of Northern Inylchek Glacier can affect the water balance of both

lakes in a cascade manner. The notion that the 1996/1997 surge displaced enough water to induce a jökulhlaup in December 1996 forms a key part of our analysis.

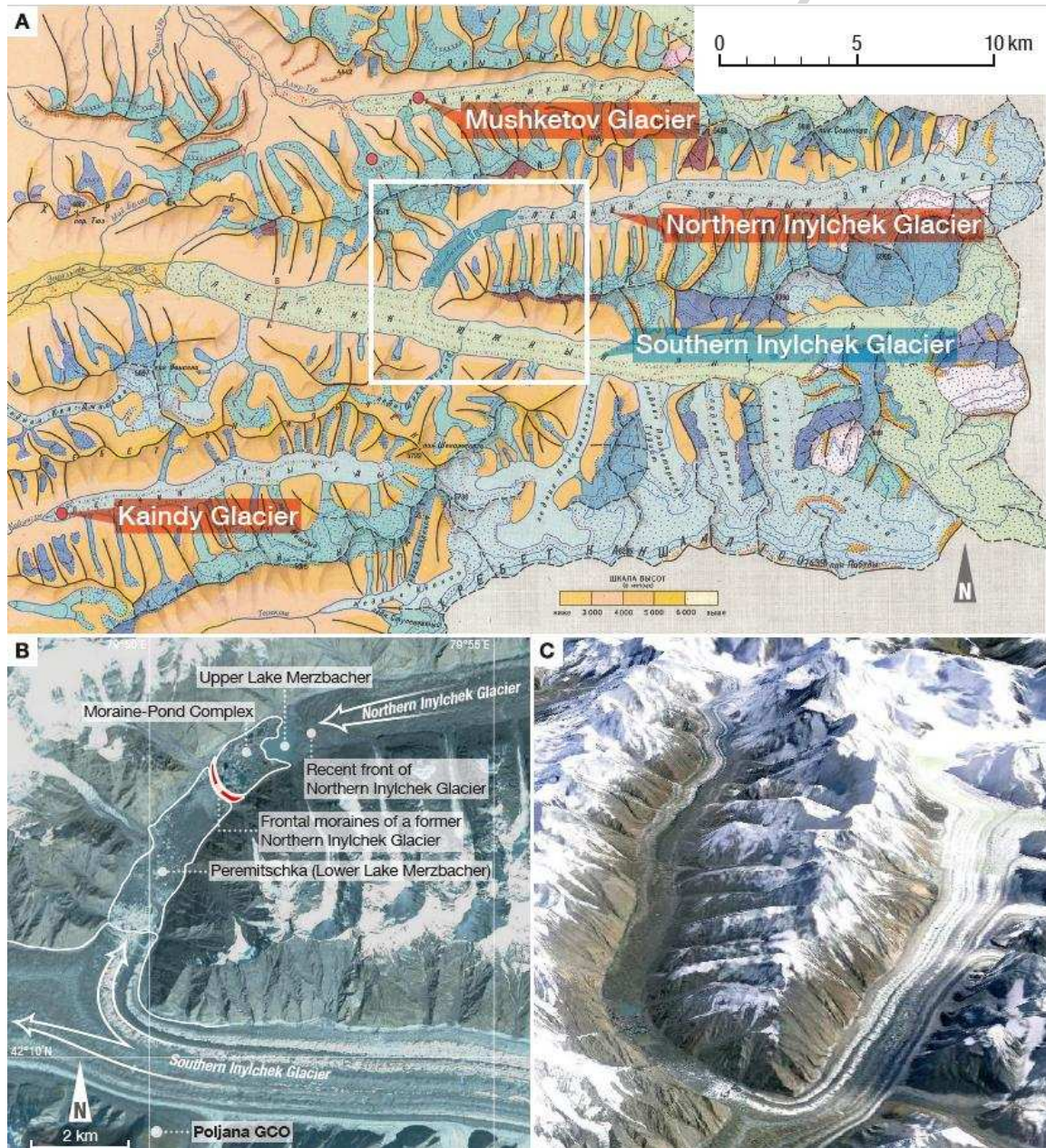


Fig. 2: (A) Map of study area, in the central Tien Shan. The box locates area of panel B. (B) Google-Earth (2013) satellite image of the confluence region of the valleys occupied by Northern and Southern Inylchek Glaciers, showing key places and features discussed in the text. (C) Oblique east-looking view (Google Earth, 2013) of the Inylchek system.

2. Study area

Our study area includes Northern Inylchek Glacier and the area immediately downvalley from it (Figs. 2 and 3) as far as the confluence of the two Inylchek valleys, where a limb of Southern Inylchek Glacier flows north (Neelmeijer et al., 2014). Two lakes exist in this area: (i) Upper Lake Merzbacher, a proglacial lake at ≈ 3300 m above sea level (asl) normally in contact with Northern Inylchek Glacier; and (ii) Lower Lake Merzbacher (≈ 3250 m asl), a marginal lake dammed by Southern Inylchek Glacier (Figs. 2B,C). The latter lake was discovered by Gottfried Merzbacher (1905) during his expedition.

The modern-day equilibrium line altitude (ELA) for glaciers in the central Tien Shan is 4400-4500 m asl (Solomina et al., 2004; Kotlyakov et al., 2010) and 4476 m asl for Southern Inylchek Glacier (Aizen and Aizen, 1997). However, trim lines in the Inylchek valleys indicate that they had been glacierized to greater depths and extents during the late Quaternary, with paleo ice-surface elevation in Southern Inylchek Valley as much as 70 m higher than now (Meiners, 1997; Blagowischinski et al., 1998). Hence it is inferred that the lakes formed after Northern Inylchek Glacier separated from Southern Inylchek Glacier. This disintegration is estimated to have occurred in the mid- or late-nineteenth century (Blagowischinski et al., 1998; Glazirin and Popov, 1999).

Of emerging scientific interest is the apparently different flow dynamics of the two Inylchek glaciers. Comparison of modern remote sensing imagery and photographs taken by Merzbacher (1906) suggests that the configuration and length (≈ 60 km) of Southern Inylchek Glacier have not changed much for over a century. In contrast, Northern Inylchek Glacier is known to have fluctuated over the same timescale, retreating significantly between 1943 and 1990 (section 2.2). Our analysis of the 1996 surge (section 4) and bathymetric study of the upper lake (section 5) extend this picture of change.



Fig. 3: (A) Oblique Google-Earth (2014) view, looking south-west, of Upper Lake Merzbacher, Peremitschka, and Lower Lake Merzbacher. (B) The Lower Lake in high-water, pre-flood condition in July 2004 (photo courtesy of Marc Roussel). (C) The lake in August 2009 after a jökulhlaup. Photographs B and C were taken from Peremitschka at a position near the dot in panel A.

2.1. Northern Inylchek Glacier

Northern Inylchek Glacier is about 32.8 km long currently (Fig. 2). Kotlyakov et al. (2010) reported its area (including tributaries) to be 181.2 km², of which 37.6 km² is debris covered. Its longitudinal surface profile from the 7000-m Khan Tengri and surrounding peaks to the snout (by Upper Lake Merzbacher) consists of firn fields above \approx 4750 m asl, intermediate stretches some 10 km long of 3-6° slope, and a main trunk \sim 20 km long with a 1.5-2° slope. The trunk spans the lowest \sim 700 m of the glacier elevation range and lies in the ablation area.

The trunk's configuration in 2015 is shown in Figure 4. It occupies an east-west oriented valley about 1 km wide and narrows slightly in the last few kilometres toward the snout. In terms of supraglacial texture and morphology, it has distinct eastern and western parts. The eastern, upper trunk displays long medial moraines that, together with input of ice from active tributary glaciers from the north and south, create a pattern of alternating bright and dark bands on the surface; crevasses are abundant here. The western lower trunk is almost completely debris covered and has few crevasses and many supraglacial ponds. Here, tributary glaciers do not intrude far into the trunk; numerous hanging

glaciers feature on the northern slopes of the valley, but their termini lie high above the trunk.

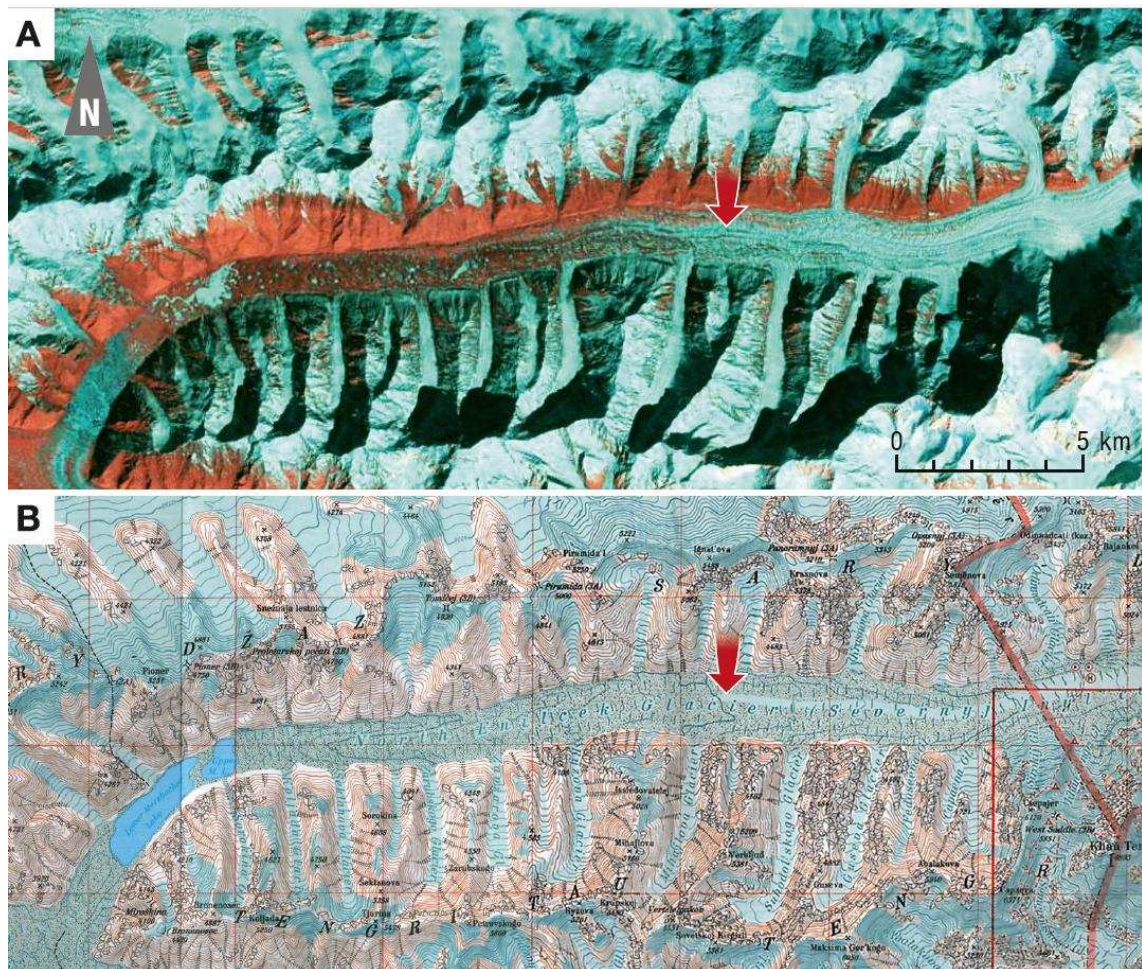


Fig. 4: Northern Inylchek Glacier. (A) Landsat 8 image acquired on March 23, 2015 (source: USGS Earth Explorer; spectral bands 6/5/4, ground resolution 30 m). The false colour image shows rocky material in a darker tone. (B) The same area on German Alpine Club 1:100.000 map, sheet 0/15, Khan Tengri (modified from Deutscher Alpenverein, 2011; map courtesy of Österreichischer und Deutscher Alpenverein). Arrow in both panels marks the transition described in section 2.1.

Interestingly, the transition between the two parts, which occurs at 80.05°E and ≈ 3750 m asl (Fig. 4), coincides with an abrupt deceleration in glacier velocity. Displacements derived for 2007-2010 from offset-tracking of synthetic aperture radar images (Li et al., 2013) show that surface velocities drop from $0.1\text{-}0.25$ m d^{-1} in the upper trunk to nearly zero downglacier of the transition; thus the lower trunk today is effectively stagnant. A similar velocity distribution was found previously by correlating Landsat images from 2006 to 2007 (Nobakht et al., 2011). Recently, Shangguan et al. (2015)

estimated surface elevation change for Northern Inylchek Glacier at coarse-time resolution by differencing digital elevation models derived from KH-9 Hexagon and SRTM3 data. They found that between 1975 and 1999, the upper trunk (between 12 and 21 km from the snout) had thinned by ≈ 100 m, whereas the last 10 km of the lower trunk thickened by ≈ 150 m (at mean rates of several m a^{-1}) across the same period and thinned in the subsequent years. Following the findings of Mavlyudov (1997) and Häusler et al. (2011), Shangguan et al. (2015; their Fig. 5) surmised the thickening to have resulted partly from the 1996 surge.

As can be seen in Figure 4A, a bright sinuous tongue of ice on the northern side of the trunk (roughly parallel to the right-lateral glacier margin) extends through the transition. This feature seems to derive from merging of flow from several northern glacier tributaries east of the transition. Its western continuation is dissected heavily by supraglacial meltwater streams. The feature - hereafter termed the worm - will be used in our analysis of the surge.

Geophysical measurements have not been made on the glacier to study its internal structure, so its thickness and thermal regime remain practically unknown. Tentatively, use of the plasticity-based glacier thickness inversion method of Li et al. (2012), assuming a surface slope of 1.5° and basal yield stress of 50 kPa (a conservative low estimate), constrains the trunk thickness to at least 200 m. We have not applied the elaborate inversion method of Farinotti et al. (2009) as it requires us to make assumptions for vertical gradients of apparent mass balance that are uncertain because Northern Inylchek Glacier exhibits unsteady flow (e.g., surge) and its trunk is heavily debris covered.

Various studies have acknowledged a surge by Northern Inylchek Glacier during the mid-1990s or described this surge generally (e.g., Mavlyudov, 1997, 1998; Blagowischinski et al., 1998; Leber et al., 2009; Häusler et al., 2012b,c; Pieczonka and Bolch, 2015) but not treated it in detail. Past examination of aerial photographs and

remote sensing imagery showed that the surge did not leave behind distinctive structural imprints such as looped or contorted medial moraines (Häusler et al., 2012b,c; Shangguan et al., 2015), which are often seen on other surging glaciers.

2.2. Proglacial area of Northern Inylchek Glacier, Peremitschka, and Lower Lake Merzbacher

Figure 2B (dated 2013) details the area between Northern Inylchek Glacier and Southern Inylchek Glacier. Several distinct morphological units relevant to our analysis are recognizable here. First, in contact with the snout of Northern Inylchek Glacier is Upper Lake Merzbacher. By mapping its area and glacier position from aerial imagery, Mavlyudov (1997) showed that the lake expanded as Northern Inylchek Glacier retreated from 1943 to 1990, while maintaining contact with the glacier. He also undertook fieldwork to measure the lake bathymetry in 1990, which we use in section 5.

The upper lake is bounded at its western limit by a moraine complex. This complex consists of hummocky moraines deposited by previous advances of Northern Inylchek Glacier and hosts many ponds, kettle holes, and the outlet stream from the lake. At its downvalley end are two 25-m-high arcuate end moraines. Aerial photographs and satellite images between the 1940s and today (Häusler et al., 2012a, 2014) show that the complex - its pattern of slopes, kettles and ponds - has not changed significantly over this period.

Between the arcuate moraines and the ice-dam of Southern Inylchek Glacier lies Peremitschka (Figs. 2B and 3), a 4.5-km-long, gently southwestward dipping plain. Here, marginal exposures along the stream leading from the upper lake revealed fine-grained lacustrine deposits (Häusler et al., 2014) overlying stagnant and decaying dead-ice (Häusler et al., 2010). Elsewhere on Peremitschka, a similar stratigraphy has been inferred from geophysical measurements that detected a low resistivity layer ($<50 \Omega\cdot\text{m}$) several metres thick overlying a very high resistivity layer (up to several tens of thousands $\Omega\cdot\text{m}$;

Scheibz et al., 2009; Häusler et al., 2011). The preceding authors interpreted the dead-ice as the remnant of the part of Northern Inylchek Glacier that separated from Southern Inylchek Glacier. By performing radio-echo sounding on Peremitschka, Macheret et al. (1993) estimated the buried ice to be 66 m thick.

Peremitschka constitutes the bed topography of Lower Merzbacher Lake. This lake receives meltwater from Northern Inylchek Glacier via the upper lake and likely also from Southern Inylchek Glacier, plus melting of ice calved from its dam and precipitation (Mavlyudov, 1997; Ng and Liu, 2009). The lake thus fills over time, most rapidly during summer. When its water depth reaches a high threshold value, typically in the range of 60 to 100 m (Ng and Liu, 2009; Kingslake and Ng, 2013a), an outburst flood (jökulhlaup) is initiated and lake-water drains through Southern Inylchek Glacier subglacially or englacially to enter the Inylchek River and then into the Sary-Djaz River. The ensuing flood duration is often one to several weeks. Typically each outburst drains Lower Lake Merzbacher completely and leaves behind icebergs on Peremitschka (e.g., Figs. 3A and 3C). Lake refilling restarts as soon as the flood paths within Southern Inylchek Glacier have sealed off sufficiently. This can occur within a week or two after flood termination, as we witnessed during our fieldwork in 2005.

More than 70 jökulhlaups from Lower Lake Merzbacher have occurred since the 1930s with a mean recurrence interval of ≈ 1 year (Ng and Liu, 2009), as known from witness accounts and river-discharge records at the gauging stations at Inylchek in Kyrgyzstan (60 km downstream of the lake) and at Xiehela in China (≈ 200 km downstream; Liu, 1992; Glazirin and Popov, 1999; Ng et al., 2007; Ng and Liu, 2009; Glazirin, 2010; Fig. 1). The year 1996 purportedly had two jökulhlaups (Mavlyudov, 1998). A first outburst was reported by border guards near Inylchek Town, although its timing is uncertain (B. Mavlyudov, pers. comms.). The second outburst occurred in late November/early December. Its recorded date of peak flow at Xiehela Station is 5

December, 1996. This outburst is unusual given low meltwater supply to the lake during winter (Ng and Liu, 2009). In section 4.2, we argue that it was triggered (or preconditioned to trigger) by displacement of water from the Upper Lake into the Lower Lake during the surge. When considering water storage and transfer in this cascade, we will use the flood volume derived from Xiehela station because published flood-hydrographic data from Inylchek station are available only for 1962–1965 and 1980–1981 (Glazirin, 2010) and 1982–1987 (Konovalov, 1990).

3. Materials and methods

In this study, we used remote sensing imagery to determine the time sequence of retreat and advance of Northern Inylchek Glacier and its interaction with Upper Lake Merzbacher by following well-established procedures (e.g., Kargel et al., 2005). We also undertook field measurements to assess changes in the depth of the Upper Lake.

3.1. Remote-sensing methods

The remote sensing data used (Table 1) consists of 40 geocoded scenes acquired by airborne and space-borne platforms between 1943 and 2011. As far as we know, they represent an essentially complete collection of usable (e.g., cloud-free) images for our purpose.

Orthorectification of the aerial photographs (from the former Soviet Union) was unfeasible because camera parameters such as calibrated focal length were not known. We georeferenced them by using geocoded satellite images, namely a QuickBird-2 scene acquired on 11 September, 2005 as well as World Imagery Base maps of ArcGIS Online Map Service (ESRI). In this process, prominent landmarks were chosen as ground control points; between 50 and 150 points were used for each aerial photograph. We used

additional ground control points located by hand-held GPS during fieldwork. These resulted in a positioning accuracy on the order of 5 m for the satellite images. Declassified Intelligence Satellite Photography (DISP) scenes such as Corona, Aragon, and Hexagon, do not need georeferencing as their corner coordinates are known. Our processing of multispectral scenes involved the standard combination of spectral bands and image enhancement (stretching of contrast ratio, dynamic range, and radiometric corrections); all Landsat scenes were pan-sharpened. Aerial photographs and satellite images were processed in ESRI ArcGIS version 9.3.

Table 1: Aerial photographs and remote-sensing images used to infer the evolution of Northern Inylchek Glacier, their date of acquisition, sensor platform and estimated ground resolution. Labels A to L refer to key stages analysed in the text.

Sensor platform	Label	Date	Ground resolution	Sensor platform	Label	Date	Ground resolution
Aerial photo		1943-07-04	~5.0 m	Landsat TM		1990-09-10	30.0 m
Aerial photo	A	1943-08-18	~5.0 m	SPOT-3, Pan	G	1996-09-12	10.0 m
Aerial photo	B	1956 (July)	~4.0 m	SPOT-3, Pan	H	1996-10-07	10.0 m
KH-2 Corona		1960-12-07	~9.0 m	JERS-1, VNIR	I	1996-11-08	18.0 m
KH-5 Aragon		1963-08-29	~9.0 m	IRS-1C Pan	J	1997-06-06	5.0 m
KH-9 Hexagon		1963-11-19	~9.0 m	Landsat 7		1999-07-09	15.0 m, pansharpened
KH-4A Corona		1965-07-20	~9.0 m	Landsat 7		2000-01-17	15.0 m, pansharpened
KH-4A Corona		1966-02-11	~9.0 m	Landsat 7		2000-02-18	15.0 m, pansharpened
KH-4A Corona		1966-09-21	~9.0 m	Landsat 7		2000-03-21	15.0 m, pansharpened
KH-4A Corona		1966-11-14	~9.0 m	Landsat 7		2000-03-24	15.0 m, pansharpened
KH-4A Corona	C	1967-08-08	~9.0 m	Landsat 7		2000-07-27	15.0 m, pansharpened
KH-4A Corona		1968-09-26	~9.0 m	Landsat 7		2000-08-12	15.0 m, pansharpened
KH-4A Corona		1970-12-01	~9.0 m	Landsat 7		2000-09-13	15.0 m, pansharpened
KH-9 Hexagon	D	1973-04-18	~9.0 m	Landsat 7		2000-10-31	15.0 m, pansharpened
KH-9 Hexagon		1973-11-19	~9.0 m	Landsat 7		2002-08-18	15.0 m, pansharpened
KH-9 Hexagon		1974-11-16	~9.0 m	ASTER		2003-06-25	15.0 m
Landsat MSS		1977-05-20	60.0 m	Quickbird	K	2005-09-11	0.65–1.0 m
Aerial photo	E	1981-11-20	~3.0 m	Landsat 7		2006-08-13	15.0 m, pansharpened
Landsat TM		1989-01-18	30.0 m	Landsat 7		2009-07-20	15.0 m, pansharpened
Aerial photo	F	1990-07-29	~3.0 m	RapidEye	L	2011-07-04	5.0 m

The aerial photographs are generally superior to the other images in terms of ground resolution because they can resolve down to 3 to 5 m. Although only digital scans of their hard copies are at our disposal, their dynamic range allows clear portrayal of surface textures. The 2005 Quickbird image has a comparable resolution. In contrast, the DISP scenes from the 1960s and 1970s have a ground resolution of 3 to 9 m. A few KH-5-, KH-9- and Landsat MSS-scenes with poorer ground resolution, and Landsat TM- and Landsat

7-scenes with the striping problem, also yielded useful information on lake and glacier configurations.

The imagery was used for visual delineation of glacier and lake boundaries and interpreting sequences of changes. Supraglacial textures and morainic features were also examined for the evolution of structural assemblages on Northern Inylchek Glacier. In numerous instances, they allowed feature tracking to estimate trunk flow velocity. The lack of stereo image pairs in 1996-1997 means that we cannot calculate how the glacier longitudinal profile evolved in the surge, but qualitative information about surface elevation changes can be gathered from some images. Remote sensing data were not used to derive digital elevation models nor the history of jökulhlaups. We assess the relationship between the latter and changes on Northern Inylchek Glacier by using published flood dates.

3.2. Field methods

Bathymetric measurements of the Upper Lake Merzbacher were made by us in 2005 and 2011 (after the surge). In 2005, water depths were measured on 2 August by an echo sounder with GPS capability (Garmin 235 Fishsounder) fixed underneath a kayak, and verified by a handful of manual plumb-line measurements. In 2011, initial echo sounding failed due to high turbidity of the lake water; instead, a meter stick was used to measure the lake depth manually on 18-19 August 2011, with each measurement point located with a hand-held GPS. The bathymetric maps in Figs. 10 C and D were compiled from these datasets by three-dimensional kriging interpolation.

4. Historical changes of the Northern-Inylchek glacial system, 1943-2011

We now describe the reconstructed variations of the glacier and lake from present day back to the mid-twentieth century. See Kopecny (2014) for an initial reconstruction, on which the current work is based.

4.1. Pre-surge period: 1943 to 1996

Figure 5 documents key stages (A to F) of the system before surging began in 1996. The sequence, covering 1943 to 1990, indicates overall retreat of Northern Inylchek Glacier and expansion of Upper Lake Merzbacher. As reported by Mavlyudov (1995) and Blagowischinski et al. (1998), ground-based photographs dated before our earliest imagery show that in 1932, the glacier snout had bordered the moraine complex. Our first image (Fig. 5A) shows a small Upper Lake Merzbacher with an area of $\approx 0.14 \text{ km}^2$ in August 1943. The moraine-pond ensemble and the lake's outflow channel are also visible, although they appear to have been partially inundated by summer high-water conditions. The glacier trunk, with a near-complete debris cover, displays many large supraglacial ponds and a hummocky surface texture that suggests a low surface gradient.

By stage B, the snout had retreated by $\approx 1.3 \text{ km}$ (i.e. mean retreat rate of 100 m a^{-1} over 13 years) and the lake area increased to 1 km^2 . By tracking supraglacial ponds identifiable on the 1943 and 1956 images, we estimate that the part of the glacier trunk visible in these images displaced by 100 m downvalley in 13 years. The corresponding mean flow speed, $\approx 0.02 \text{ m d}^{-1}$ (7.7 m a^{-1}), is an order of magnitude less than that measured by Li et al. (2013) for the upper trunk today.

Subsequent images in the presurge period (Fig. 5; stages C to F) show continued glacier retreat and lake expansion; no significant glacier readvance occurred until the 1990s. This behavior is consistent with a slow-flowing, debris covered trunk that downwasted passively by differential ablation and whose retreat was probably enhanced

by strong frontal ablation caused by the contact with proglacial lakewater. Our inference of the trunk's near-stagnancy is corroborated by the few icebergs on the lake in all four stages, which indicate limited frontal calving.

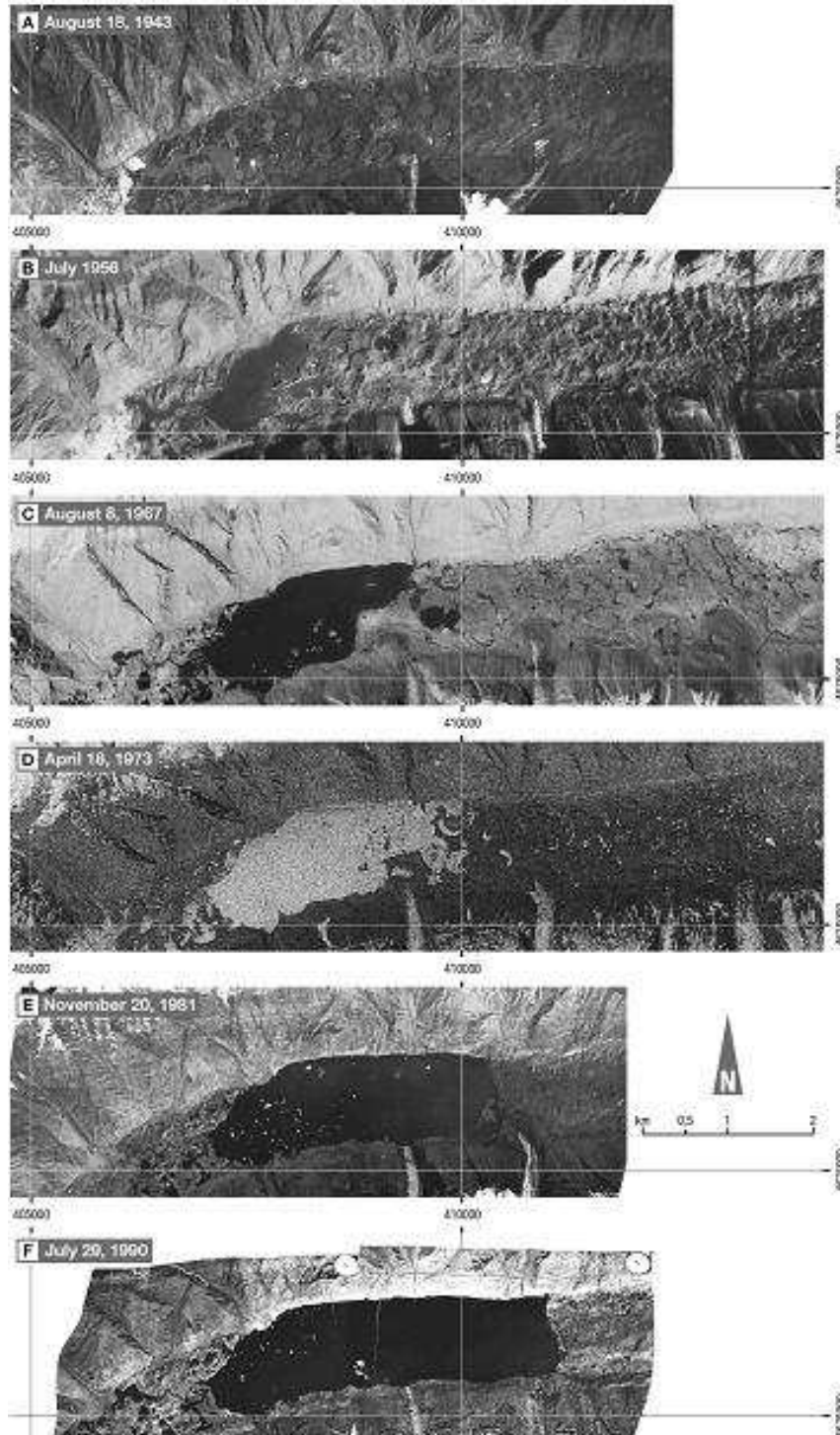


Fig. 5: Georeferenced aerial photographs and satellite images of Upper Lake Merzbacher and Northern Inylchek Glacier from 1943 to 1990, showing stages A to F discussed in the text. See Table 1 for details about the images. Reference lines indicate UTM coordinates.

The images from the mid-1950s to mid-1970s show that the lake had developed a longer arm on its northern part, reflecting faster retreat of the right-lateral glacier front margin. A possible reason of this is more intense solar radiation reflected off the northern slopes and less shadowing there compared to left-lateral margin. The arm had disappeared by 1981 (Fig. 5E). The lake's western shoreline, confined by the moraine complex, remained roughly stationary from 1956 to 1990. This stability suggests that either the complex is not predominantly ice-cored or its upper ice-free horizons are thick enough to protect buried ice from melting under contemporary (nonpermafrost) conditions. We favour the latter interpretation because thick subsurface ice is found farther west in Peremitschka (section 2.2).

By July 1990 (Fig. 5, stage F) the Upper Lake had grown to be ≈ 4 km long and ≈ 1 km wide, with its northern and southern shores fit against the valley flanks. Its area was 3.8 km^2 , similar in size to a nearly full, contemporary Lower Lake Merzbacher. This was the maximal recorded extent of the Upper Lake in the twentieth century.

Feature-tracking across stages E and F yielded trunk displacements of 100-200 m and thus mean ice-flow speeds of $0.03\text{-}0.06 \text{ m d}^{-1}$ ($11\text{-}22 \text{ m a}^{-1}$) between 1981 and 1990. Therefore near-stagnancy of the lower trunk had continued until the early 1990s. We examined also the position of the worm (the sinuous tongue described in section 2.1; Fig. 4A) during the presurge phase. Its frontal part, identifiable by bright texture, was visible in July 1956 (Fig. 5B) and persisted through the images of 1965, 1966, and 1967 (Fig. 5C). Prior to the surge in 1996, its front-edge position had remained stable for 40 years.

There are no high-resolution, pre-1996 images of Northern Inylchek Glacier in the area farther east of that shown in Fig. 5, so we cannot evaluate the flow speeds and features on the upper trunk that might show a buildup toward a surge or signs of a developing surge bulge and any associated thickening.

4.2. The surge phase and afterward: 1996 to 2011

The next images, covering 1996 to 2011, document drastic changes on the glacier - its speedup and readvance, which we interpret as a surge starting in September/October 1996 and perhaps lasting into 1997, followed by return to quiescence, downwasting and frontal retreat.

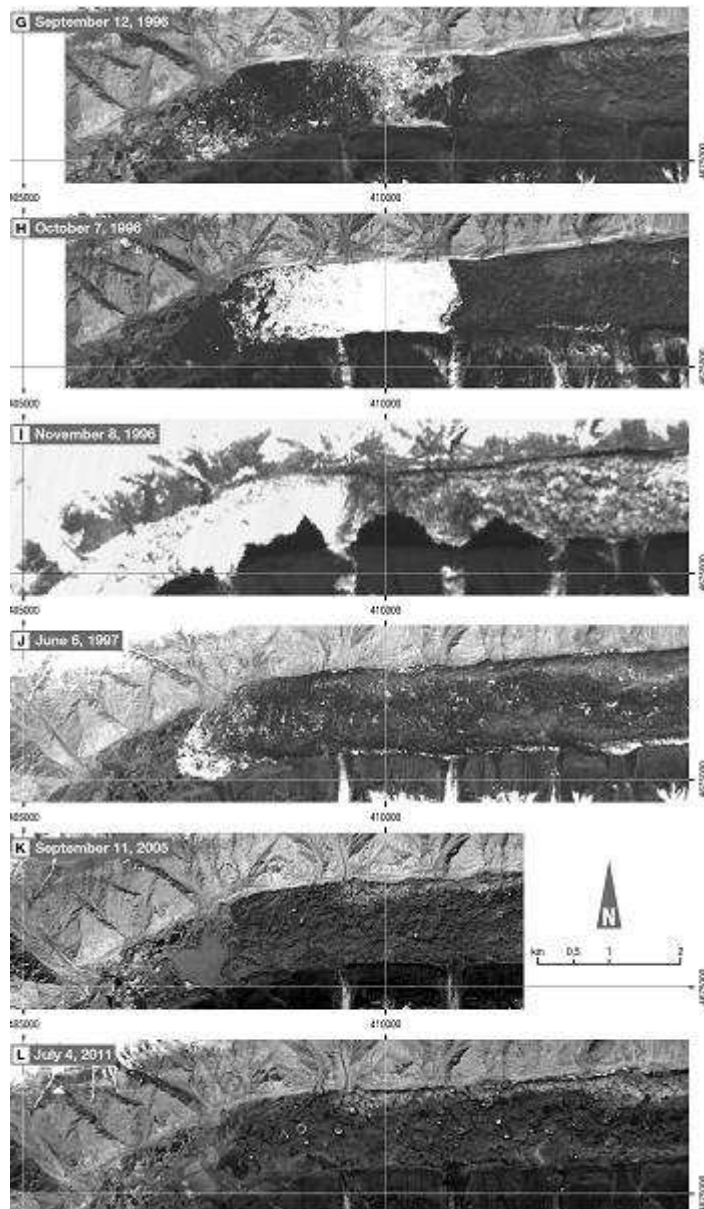


Fig. 6: Satellite images of Upper Lake Merzbacher and Northern Inylchek Glacier from September 1996 to July 2011, showing stages G to L discussed in the text. See Table 1 for details about the images. Reference lines indicate UTM coordinates.

Figure 6 outlines key stages of this sequence. (Detailed geomorphological interpretations are postponed to section 4.2.2.) The first image, from 12 September, 1996

(Fig. 6, stage G) shows a snout position similar to that in July 1990 (Fig. 5, stage F), which implies interruption of the trend of glacier retreat and lake expansion of the previous decades. Both images in stages F and G feature the worm. Its tip had moved down-glacier by about 400 m from 1990 to 1996, implying a mean flow speed of 0.18 m d^{-1} (several times on the 1956-1990 average) for the period. This reactivation of glacier flow is probably what halted the snout retreat and is consistent with more icebergs seen on the Upper Lake in stage G. The worm is also visible in the next image taken 25 days later on 7 October, 1996 (Fig. 6, stage H). By this time it had displaced by another 250 m, and the lake seems to be choked with icebergs; the inferred mean flow speed (over the 25 days) is 10 m d^{-1} (3.65 km a^{-1}). This observation removes any doubt that the trunk was accelerating into a surge by early October. The interval between stages G and H shows the first sign of westward snout advance by $\approx 250 \text{ m}$, at a mean rate of $\approx 10 \text{ m d}^{-1}$ (same as the mean trunk flow speed for the interval).

Two more images taken on 8 November, 1996 and 6 June, 1997 (Fig. 6, stages I and J) constrain the rigorous phase of the surge. The former has lower but sufficient quality for us to estimate how far the snout advanced during the intervals H to I (32 days) and I to J (210 days). Its displacement in the interval H to I was 1600 m, yielding a mean advance rate of 50 m d^{-1} . Between stages I and J, a farther snout advance of $\approx 1850 \text{ m}$ took place, nearly eliminating the Upper Lake; the corresponding mean advance rate was 9 m d^{-1} . The surge thus seems to have abated in the second interval. By June 1997 (stage J), the lake had effectively been overridden; what remained of it appears in Figure 6J as a small, iceberg-strewn (bright-textured) area east of the moraine complex; and the most active phase of the surge can be considered to have ended because the snout was only $\approx 100 \text{ m}$ behind its most extended position seen by an expedition in August 1997 (section 4.4). Imagery between stages I and J is lacking for pinpointing when and how fast the snout

reached its June 1997 position. By evaluating different scenarios for this part of the snout's history, we argue later (in section 6.3) that it arrived there well before this date.

The next available image, a Landsat 7 scene captured in July 1999, reveals the glacier back in its quiescent state. Then the snout had retreated and the trunk began down wasting; the Upper Lake was about 600 by 700 m in size ($\approx 0.35 \text{ km}^2$ in area). Images acquired later between 1999 and 2005 indicate more snout retreat and lake areal growth to 0.55 km^2 . The images in stages K and L (Fig. 6) support our interpretation that the active surge phase ended before June 1997 because features on the trunk (supraglacial ponds and the worm) in these images show negligible downvalley displacement since stage J.

4.2.1. Triggering (or hastening) of the 1996 outburst of Lower Lake Merzbacher by the surge

As mentioned before, a jökulhlaup caused by the outburst of Lower Lake Merzbacher occurred in December 1996, peaking in discharge at Xiehela station on 5 December (section 2.2). It happened in the early part of the declining surge phase between stage I (8 November, 1996) and stage J (6 June, 1997). The estimated floodwater volume released by the lake was $2.84 \pm 0.09 \times 10^8 \text{ m}^3$, excluding background baseflow and water contribution from Southern Inylchek Glacier that had been subtracted during flood-hydrograph separation (Ng and Liu, 2009). Given a time delay of 1-2 days for the flood wave to propagate downriver from the lake and Southern Inylchek Glacier to Xiehela (Ng and Liu, 2009; pers. comm. with G. Glazirin), we infer that peak flood discharge from the lake occurred on around 3 December. Also, the typical duration of the rising phase of jökulhlaups from this lake, about 1-2 weeks (section 2.2), allows us to trace the probable time of flood initiation to be earlier still: in late November. (We necessarily distinguish between (i) the flood duration and (ii) travel time of the flood downriver in these considerations). From the start of the surge in September/October to November, the

glacier must have displaced water from the Upper Lake into the Lower Lake because its surge was overriding the Upper Lake (last section). Here we connect these events and argue that the resulting water input into the Lower Lake had triggered the outburst - or preconditioned it to happen earlier - by raising the lake level rapidly.

This idea is plausible because the rate of water input exceeds other meltwater sources feeding the Lower Lake during autumn/winter. In the 32 days from stage H to I, the snout advance of 1600 m together with 1990 bathymetry data for the Upper Lake (section 5) yields an estimated displaced water volume on the order of $1.0 \times 10^8 \text{ m}^3$, if we assume negligible surface elevation change for the Upper Lake and a parabolic lake-bed cross profile 1 km wide and 100 m deep. The corresponding mean displacement water flux for this interval, $36 \text{ m}^3 \text{ s}^{-1}$, is comparable to the measured outflow from the Upper Lake into the Lower Lake owing to glacier melt during summer (~ 31 to $52 \text{ m}^3 \text{ s}^{-1}$; Mavlyudov, 1995). As melting is suppressed in autumn/winter, the displacement flux must have then far exceeded any background meltwater discharge routed via the Upper Lake.

Even if we neglect any meltwater released by Northern Inylchek Glacier during the surge, the displaced volume of $1.0 \times 10^8 \text{ m}^3$ would fill a significant fraction of the Lower Lake basin, which has an outburst capacity on the order of $1\text{-}2 \times 10^8 \text{ m}^3$. This range estimate for the capacity derives from modelling studies that show that the Lower Lake's outburst threshold is not constant but varies from flood to flood (Ng and Liu, 2009; Kingslake and Ng, 2013b). The range also brackets the capacity $1.29 \times 10^8 \text{ m}^3$ estimated by Kuzmichenok (1983), who reconstructed the Lower Lake's bed topography using stereophotographs taken in 1982 when the lake was empty after an outburst.

Later on during the surge, from stage I to J, the volume displaced by the advancing snout is less because the Upper Lake becomes shallower in its western/distal portion, but this volume (several 10^7 m^3) would have continued to fill the Lower Lake. Accordingly,

we estimate the total water volume displaced by the surge (stage G to J) to be on the order of $1.5 \times 10^8 \text{ m}^3$. A different approach to back out this volume subtracts the residual volume of the Upper Lake in June 1997 after the surge ($\approx 0.3 \times 10^8 \text{ m}^3$, estimated using the bathymetry data in Fig. 10B) from Mavlyudov's (1995) estimate for the Upper Lake volume in 1990 ($\approx 2.6 \times 10^8 \text{ m}^3$), and gives $2.3 \times 10^8 \text{ m}^3$. Although these results differ (probably because of different assumptions for the Upper Lake crosssection), they indicate that the total surge-displaced volume can supply a significant fraction of one flood; they respectively account for 53% and 82% of the observed December 1996 flood volume.

For several reasons, it is difficult for us to determine the water balance throughout the cascade to reconstruct the (actual) filling history of Lower Lake Merzbacher up until the outburst. The initial water level/volume of the Lower Lake in September 1996 before the surge is unknown. The sizes of meltwater sources feeding the lakes during the surge (e.g., including basal water from Northern Inylchek Glacier produced by enhanced sliding) are also uncertain - an unrecorded but potentially large subglacial water pulse might have been released by the glacier at surge termination. There are suggestions also that the Southern Inylchek ice dam is leaky (Wortmann et al., 2013; Krysanova et al., 2015). Despite these uncertainties, the surge-displaced volume is clearly an extra input that must have hastened the outburst. In section 6.3, we turn these considerations to the different purpose of constraining the snout's motion between stages I and J.

4.2.2. Surface morphology of the surging trunk

We turn to examine the surge dynamics of Northern Inylchek Glacier closely by studying the evolution of glaciotectonic and geomorphologic features on the trunk. Specifically we use the four high-resolution images from stages F, G, H, and J, which bracket the onset, intensification, and recession of the surge. Figure 7 shows zoomed areas of these images, with landmarks added to aid analysis. These landmarks include a rock pedestal on the

glacier's right lateral margin (circled), a fixed UTM position **1** located where a northern valley meets the trunk, and another fixed UTM position **2** near where a southern tributary glacier meets the trunk. In Figure 7, the right-hand column highlights our mapping and interpretation of key features.

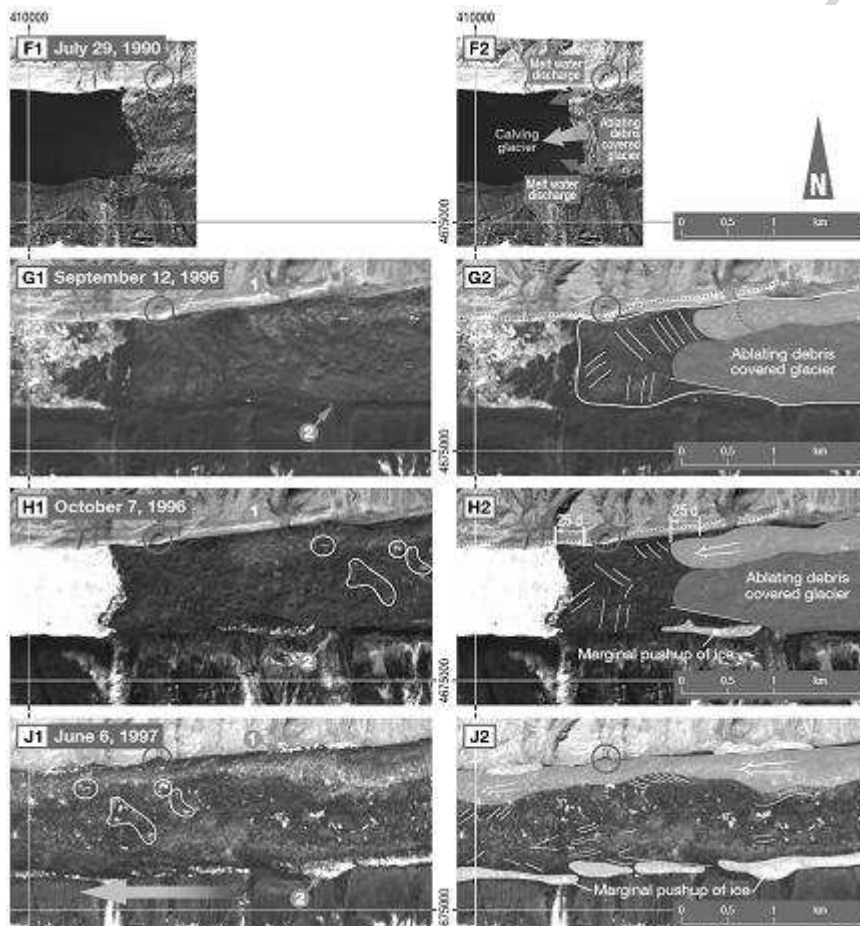


Fig. 7: Identification of flow textures and landforms on Northern Inylchek Glacier across stages F, G, H and J. Both columns show the same enlarged portions of the corresponding images. The right column highlights our mapping and interpretation; see section 4.2.2 for an explanation of key landmarks (the circle and locations 1 and 2 near the glacier margin). Reference lines indicate UTM coordinates.

Stage F: The July 1990 image (Fig. 7, F1 and F2) covers only a kilometre-long section of the trunk as no images farther east are available. It shows numerous long transverse crevasses within several hundred metres of the snout that reflect longitudinal extension of the ice flow there; also, the ice front is scarp-like. These features may have been caused by contact of the front with lakewater that is relatively deep: 80-100 m according to Fig. 10B (section 5). However, data on the glacier's thickness are lacking, so whether its

frontal section was afloat or grounded cannot be deduced. The crevasse orientation favours calving, but the image shows no icebergs on the lake nearby except for a few floating in its western part (Fig. 5F).

Stage G: As reported before, the September 1996 image signals reactivation of trunk flow interrupting the long-term snout retreat. In stage G (Fig. 7G), the snout is no longer sharply defined, and icebergs abound on the eastern side of the Upper Lake. The trunk surface has also changed significantly since stage F, and now shows three distinct units. Nearest to the snout is an area of $\sim 1 \text{ km}^2$ with numerous crevasses, many hundreds of metres long, that form a chevron pattern and dissect the area into elongated blocks. Crevasses by the northern glacier margin are oriented NW-SE, whereas the few by the southern margin are oriented N-S. We interpret this pattern as evidence of brittle deformation across the area and strong lateral shear stress exerted by the valley flanks on the trunk, which is consistent with flow reactivation. Farther upglacier are two other units with markedly fewer crevasses. The southern unit is an intensely debris covered area with many supraglacial ponds. The northern unit is the worm. Its frontal position between 1956 and 1974 is marked by the dotted line in Fig. 7G. By stage G it had moved downvalley by 500 m, but because of the long time gaps between remote sensing images before September 1996, when it had begun advancing is unknown.

Stage H: The next image (Fig. 7: stage H; 7 October, 1996) documents snout advance by 250 m and trunk acceleration to $\sim 10 \text{ m d}^{-1}$ since stage G. Despite the transition into surging, the three units have not changed their overall configuration. A new observation is a prominent curvilinear ice ridge sheared off the left-lateral trunk margin along the 1-km stretch west of landmark **2**. Its formation is not surprising because this part of the valley narrows at an angle of $\sim 3^\circ$, so the trunk's forward motion must cause lateral compression

that pushed material onto the sides. A white speck in the image of stage G suggests that this process was active 25 days earlier.

For the interval G to H, feature tracking (of the worm and supraglacial depressions) shows that the lower trunk displaced by a similar amount (≈ 300 m) across its entire width. Such plug flow suggests that significant basal sliding dominated the glacier's longitudinal velocity distribution. The snout advanced less far (≈ 250 m), so a frontal area of roughly $50 \text{ m} \times 1 \text{ km}$ must have ablated and/or calved into the Upper Lake. Calving had certainty occurred because Figs. 6H and 7H show near-complete coverage of the lake by icebergs.

Stage I: The very-near-infrared JERS-1 scene of 8 November, 1996 (Fig. 6I) is too low quality for detailed geomorphological analysis. However, the mean snout-advance rate of 50 m d^{-1} between stages H and I (section 4.2) imply that over this interval, the lower trunk had a minimum mean ice-flow velocity of this rate, as some frontal ablation/calving is expected to have occurred.

Stage J: By June 1997, the snout had overridden the Upper Lake, and the surge was ending or had ended. Figure 7 (J1 and J2) shows many more curvilinear sheared ice ridges along the northern and southern margins, implying that surging-induced, lateral compression had continued to act on the trunk. The trunk has noticeably thickened, as shown by the position of its right lateral margin, which now obscures an old right-lateral trimline and the rock-pedestal landmark previously visible in stage G. Considering how far this margin migrated between the images and assuming a 30° slope, the estimated thickening is roughly 40 m. The thickening is probably the combined result of lateral compression and transferral of thicker ice from upvalley.

The trunk surface in stage J consists of (i) an unbroken but uneven extension of the worm, which is relatively free of crevasses and occupies a width of 100-300 m near the

northern margin, and (ii) a darker surface elsewhere across the trunk's central and southern parts showing multiple chevron and transverse crevasses (Fig. 7, J2). The trunk surface texture has changed considerably since stage H, with the appearance of many isolated bright patches of ice reflecting the evolution of a strongly hummocky surface caused by sustained deformation and fracture. Our identification of similar features on H1 and J1 suggests that not only had the worm advanced, but the central part of the glacier also advanced by a similar distance. By correlating what appear to be identical clusters of features across the images of stages H and J (marked in Fig. 7), we estimate that this area of the lower trunk displaced downvalley by ≈ 2.7 km in the intervening 8 months. That these features straddle the trunk's width again indicates that the surge occurred as plug flow. We note that their displacement is less than the snout-advance distance of 3.45 km (section 4.2) over the same interval; in addition, the forward motion of ice near the snout must exceed this distance because some ablation/calving must have occurred over 8 months. The associated minimum strain rate, $\approx ((3.45 - 2.7) \text{ km}/3 \text{ km})/242 \text{ days} = 0.38 \text{ a}^{-1}$, far exceeds the critical strain rates for crevasse formation on glaciers ($\approx 0.1 \text{ a}^{-1}$ or less; Cuffey and Paterson, 2010). Hence, it must include a contribution from voids, and this is consistent with the ample crevasses seen on the trunk.

4.3. Brief summary

Figure 8 plots successive snout positions of Northern Inylchek Glacier reconstructed for all stages discussed above. During the pre-surge period (1943 to September/October 1996), the snout retreated by 3700 m at a relatively constant rate of 0.19 m d^{-1} . During the surge, its mean advance rate was 30 m d^{-1} between 12 September and 8 November (stage G to stage I) and as much as 50 m d^{-1} for the shorter interval from 7 October to 8 November (H to I). The snout advanced by 3700 m in total (G to J). In the 12 years after the surge, it retreated at 0.1 m d^{-1} , roughly half of its mean retreat rate before the surge.

Given (i) our inference of mean trunk flow velocities reaching $\approx 50 \text{ m d}^{-1}$ during the surge, (ii) the relatively short surge duration (certainly < 1 year), and (iii) the lack of evidence (yet) of a slow surge bulge propagating through the trunk at surge initiation, we classify the 1996 surge as being Alaskan-type, not Svalbard-type (section 1).

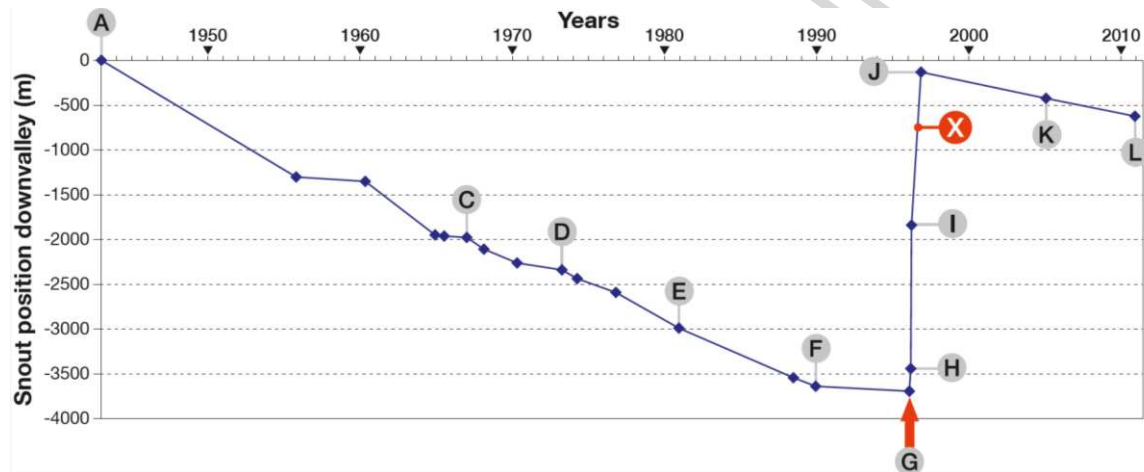


Fig. 8: Reconstructed variation of the snout position of Northern Inylchek Glacier from 4 July, 1943 (stage A) to 4 July, 2011 (stage L). The original data derive from Kopecny (2014, table 9). Distance is defined positive in the down-valley direction. Line segments are linear interpolations that do not necessarily represent the actual history. The snout's advance from stage G to stage J encapsulates the surge in 1996. Position X is discussed in section 6.3.

4.4. Glaciotectonics at the surge front in 1997

We consider next the characteristics and behavior of the snout in June to August 1997, by drawing on additional observations collected by a field expedition (Blagowischinski et al., 1998).

As described before, on 6 June, 1997 the snout was in contact with a diminished Upper Lake. Figure 6J shows an irregular snout morphology consisting of two ice lobes. Behind the snout, the glacier surface exhibits several arcuate features with similar orientation.

Figure 9 shows an aerial photograph of the snout taken by the expedition on 16 August, 1997. It identifies the area with the arcuate features as an intensely crevassed region, whose topography is dominated by concentric ice ridges that are sediment-rich and

generally convex downvalley. Farther down, closer to the snout, the ridges become more subdued in relief and contain lighter sediments. We interpret the whole system of ridges to have formed as a result of multiple thrusts dipping upglacier; some thrusts probably reached the glacier bed and transported basal (lake-bed) sediments to the surface. According to bathymetric measurements (section 5), in 1990 the lake in this area was 17-32 m deep and its bed sloped up westward. Therefore, during the surge, the advancing tongue could have eroded and deformed fine-grained lake-bed sediments on the rampart, transporting them forward. We suspect that this process produced the sediment mounds and some of the lower ridges near the snout.

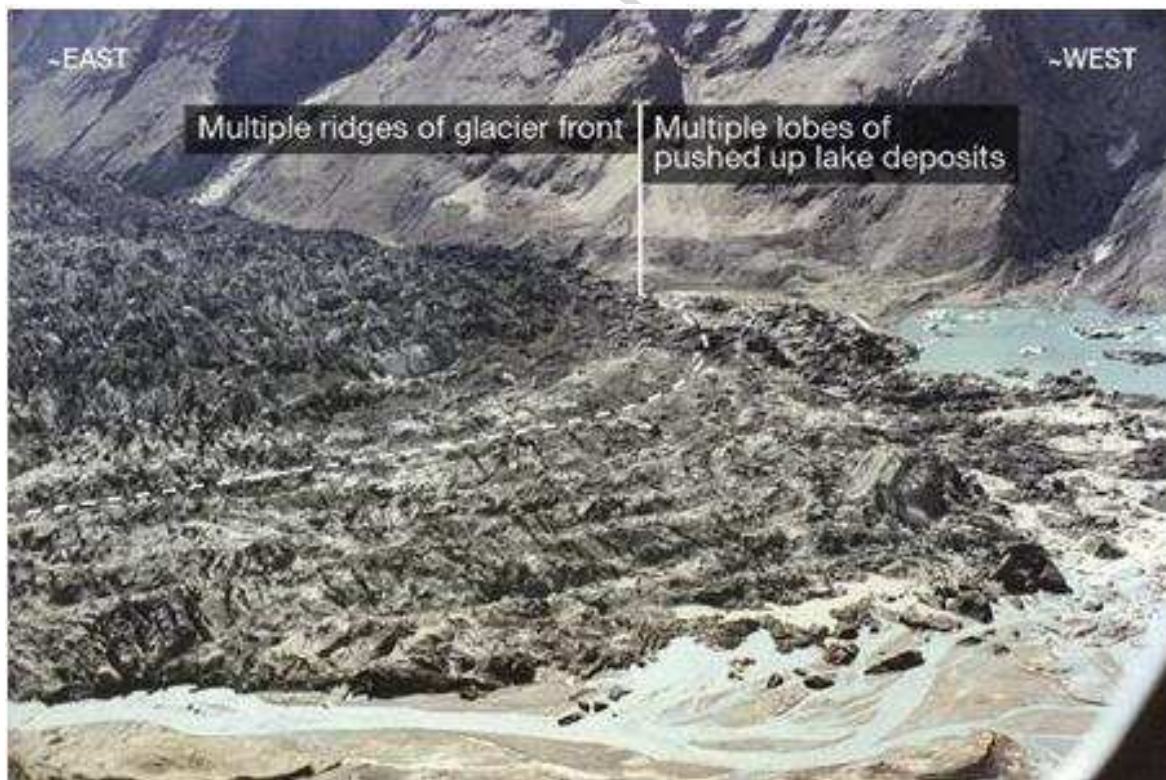


Fig. 9: Oblique view of the snout of Northern Inylchek Glacier from helicopter on 16 August, 1997, looking towards the south-east. Upper Lake Merzbacher can be seen on the far right. The tributary glacier at the top-left is Koljada Glacier. (Photograph courtesy of Gleb Glazirin)

In Figure 9, these ridges/mounds show signs of degradation, especially near the lake margin and on the left-lateral side of the snout (e.g., mid-far-right area of photograph). But some features and relief on them look relatively fresh, despite the time since the fastest part of the surge phase subsided. This observation suggests that glacier front

dynamics might still be active in 1997 summer. In this connection, Blagowischinski et al. (1998) reported that alpinists at camp Khan Tengri farther upvalley had witnessed flow activation of Northern Inylchek Glacier in June 1997. This is consistent with a snout advance of ~100 m between June and August inferred from our imagery. Speculatively, a sudden speed up or mini-surge of the glacier might have occurred in the summer, activated by seasonal meltwater being injected into the subglacial interface of the trunk. The advance could have displaced some water from the (regrowing) Upper Lake and helped trigger the outburst flood from Lower Lake Merzbacher in summer 1997, which had a recorded peak discharge date of 31 July at Xiehela station (Ng and Liu, 2009).

5. Bathymetric and areal evolution of Upper Lake Merzbacher from 1990 to 2011

Besides overriding the Upper Lake and displacing its water downstream, the surge had significant long-term impact on its bathymetry by inputting sediment into it. The data in Figure 10 illustrate this effect. Figure 10B shows the lake's bathymetry measured by Mavlyudov (1995) in 1990, the year when it attained maximal areal extent and length (section 4.1). At this time, the distal (western) part of the lake bed deepened gradually to ≈ 60 m over the first kilometre, and more steeply to ≈ 100 m over the next several hundred metres; the depth then stayed roughly at this value until near the ice front, where it reduced to 81 m. These data show that the distal bed slope averaged approximately 0.05 ($\approx 3^\circ$), although its lower part was as much as twice as steep. This was the rampart over which the snout advanced during the declining surge phase.

More recent fieldwork by us in 2005 and 2011 obtained the bathymetric maps in Figs. 10C and D. By these times, retreat of Northern Inylchek Glacier had re-enlarged the lake to nearly its present size (similar to that in Figs. 6K and 6L). Much sedimentation had occurred in the lake since 1990, as its mean depth had reduced to 8 m in 2005 and 2 m in 2011. This area was the distal part of the lake in 1990 where the mean depth used to be

≈ 20 to 30 m. If we assume that, between 1990 and the 1996 surge, the lake bed here stayed at the same elevation (limited sedimentation is suspected here because the snout lay several kilometres upvalley for most of this time), then we estimate an average ≈ 12 to 22 m of sedimentation from 1996 to 2005 and another 6 m of sedimentation from 2005 to 2011 for the area. The corresponding mean sediment deposition rates for the periods are ≈ 1.3 - 2.4 m a^{-1} and 1 m a^{-1} , respectively. The decline in rates is not surprising, because the fastest sediment input to the lake should occur immediately after the surge.

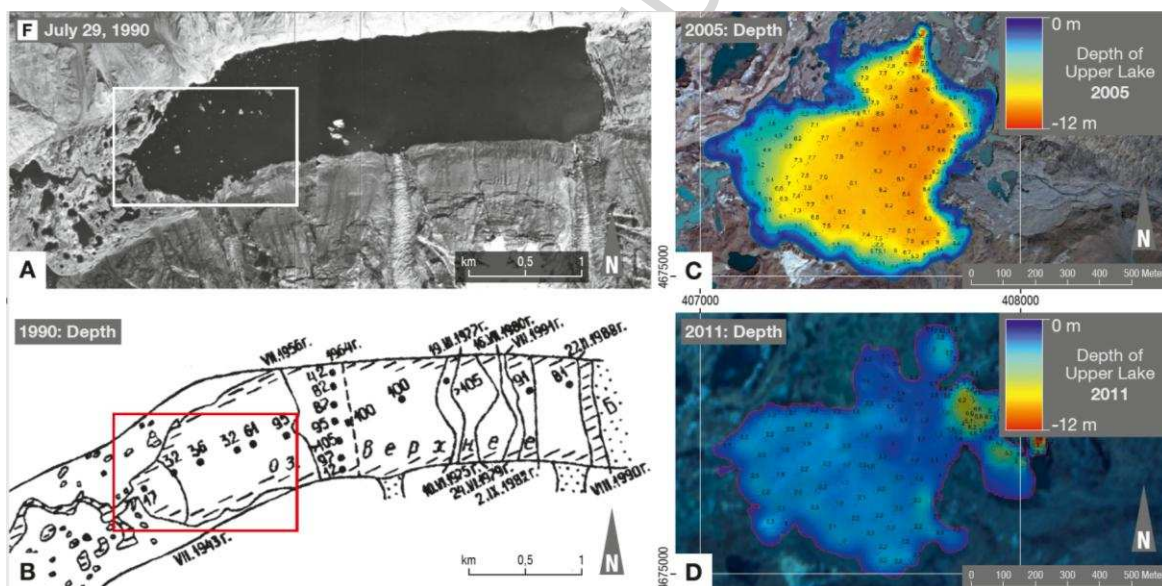


Fig. 10: Changing extent and bathymetry of Upper Lake Merzbacher. (A) Aerial photograph of the lake on 29 July, 1990 (stage F). (B) Bathymetric measurements in 1990, reproduced from Mavlyudov (1995); this panel includes his mapping of snout positions of Northern Inylchek Glacier from 1943 to 1990. (C) and (D) Colour-coded bathymetric maps of the lake on 2 August, 2005 and 18-19 August, 2011 made from our field measurements. The mean water depth was 8 metres in 2005 and 2 metres in 2011. Boxes in (A) and (B) locate the areas of (C) and (D).

These deposition rates stand out among rates recorded in proglacial lakes elsewhere. Schiefer and Gilbert (2008) cored the base of Silt Lake, a proglacial lake with an area of $\approx 0.62 \text{ km}^2$ located at 800 m asl in British Columbia, Canada, and found rates of 0.5 to 20 mm a^{-1} for the period 1989-2004. Deposits of similar thicknesses were found in Nigardsvatn ($\approx 0.5 \text{ km}^2$ in area; 285 m asl) in front of Nigardsbreen, Norway, by Kennie (2012), who estimated a mean sedimentation rate of 2 - 6 mm a^{-1} from 1979 to 1993. In

terms of depth reduction, the rates estimated for Upper Lake Merzbacher are two orders of magnitude higher than these examples.

A more objective comparison of sediment yields across glacier systems can be made by accounting for glacier catchment sizes; i.e. we compare specific sediment yields found from normalizing the total sediment mass production rate by glacier catchment area. The Upper Lake had an area $\approx 0.25 \text{ km}^2$ (in Fig. 10). If we assume a dry density of 1.6 Mg m^{-3} for its bed sediments (ballpark estimate for silty-clay sediments with 0.3–0.6 porosity), then the mean deposition rates calculated above lead to total sediment mass production rates of 5.3 to $9.8 \times 10^5 \text{ Mg a}^{-1}$ (1996-2005) and $4 \times 10^5 \text{ Mg a}^{-1}$ (2005-2011). Normalizing these results by the glacier catchment area east of the lake ($\approx 287.5 \text{ km}^2$) gives 1.9 to $3.4 \times 10^3 \text{ Mg km}^{-2} \text{ a}^{-1}$ and $1.4 \times 10^3 \text{ Mg km}^{-2} \text{ a}^{-1}$ as the specific sediment yields for the two periods, respectively. Although our calculation is based on bed-elevation change and does not distinguish different modes of sediment input (suspended load vs. bedload transport) into the Upper Lake by the surge, our yields are similar in order of magnitude to the minimum specific suspended sediment yield for Silt Lake, $1.74 \times 10^3 \text{ Mg km}^{-2} \text{ a}^{-1}$ (Schiefer and Gilbert, 2008). They also exceed the total specific sediment yields derived by Bogen et al. (2015) for Nigardsvatn ($561 \text{ Mg km}^{-2} \text{ a}^{-1}$) and another proglacial lake, Engvatnet, in Norway ($566 \text{ Mg km}^{-2} \text{ a}^{-1}$). Our findings thus illustrate the potential of significant short-term enhancement of sediment transport and deposition in glacier systems caused by the surges.

A farther inference is that the 1996 surge must have injected sediments also into Lower Lake Merzbacher (via the Upper Lake throughflow), potentially changing its bed topography, e.g., causing infilling. Such changes may be relevant to studies seeking to reconstruct the filling-outburst cycles of the Lower Lake. However, our available data do not enable an estimation of the sediment input.

6. Discussion

In this paper, remote sensing data have been used to reconstruct and analyze the dynamical and frontal histories of Northern Inylchek Glacier from 1943 to 2011, with a focus on its 1996 surge. Our treatment covers a surge cycle and extends earlier descriptions. We finish by discussing our findings in more general glaciological, hydrological, and sedimentological contexts.

6.1. Surging dynamics

The 1996 surge exhibited concerted dynamical, geometrical, and geomorphological changes in the lower trunk that clearly evidence rapid transfer of ice from upglacier lasting several months. Key observations include: (i) flow reactivation of the near-stagnant lower trunk and ice-flow acceleration by at least two orders of magnitude (≥ 50 m d⁻¹ during surge phase, versus 0.18 m/d for interval G–H and much less before that); (ii) advance of the snout by 3.7 km in total; and (iii) thickening of the lower trunk, abundant crevassing on its frontal part, and formation of sheared ice ridges at its lateral margins, during the surge (sections 4.2 and 4.2.2). The magnitude and spatial pattern of surging velocities are consistent with rapid sliding over a temperate base. Despite the time gap in our imagery collection between 1990 (stage F) and September 1996 (stage G, when the glacier transitioned into surging), we have not discerned any surge bulge propagating downglacier during surge initiation (no significant change is apparent in the lower trunk's thickness across interval F–G) that would suggest a polythermal surge (as for Bakaninbreen, Svalbard; Murray et al., 1998) or a slow surge (as for Trapridge Glacier in Yukon, Canada; Frappé and Clarke, 2007). The characteristics reported here render the 1996 surge as similar to glacier surges in the Karakoram and Alaska.

The absence of contorted or looped moraines on the surging glacier may be caused by the trunk's straight configuration and a lack of fast-flowing tributaries feeding it from

the sides, notably in its lower portion. The surge might have deformed morainic shear zones at the confluences between the trunk and some of the larger tributaries farther upvalley (e.g., near the arrow in Fig. 4), but the lack of repeat remote sensing imagery for that area precludes a study of such process. The formation history of the worm remains elusive. That this feature has a distinct downglacier end may mean that the flow of one or several northern tributaries had not invigorated or not joined the trunk until some time ago. This interpretation would imply additional flow variability within the Northern Inylchek system besides its surge dynamics. Alternatively, the worm's abrupt termination may merely reflect differences in material composition and ablation regime between it and the neighbouring areas, rather than such variability.

6.2. Surge cycle and its climatic forcing

Our analysis identifies all key phases of a typical surge cycle (e.g., Jiskoot, 2011): (i) a quiescent phase, during which the glacier snout retreated (1930s to 1996), (ii) initial build up toward a surge when the retreat is halted (September 1996 or shortly before), (iii) pre-surge phase (September to October 1996) when trunk flow began to accelerate, (iv) active surge phase (from September/October 1996 onward), and (v) deceleration and return of the trunk to quiescence (probably before the start of 1997; next section).

The inferred minimum length of the surge cycle, from 1932 when the snout lay near the moraine-pond complex, to 1997 when it regained the same position, is 65 years. We have not come across historical documentation of a previous surge of Northern Inylchek Glacier, so whether the cycle is repetitive is unknown. If one assumes continued cyclicity with a period of seven decades and no significant change in glacier dynamics and mass-balance forcings, one might speculate that the glacier last surged in the 1920s or early 1930s and will surge in the 2060s.

The 1996 surge occurred after several decades during which the long-term average mass balance of Northern Inylchek Glacier may have been negative, but its occurrence implies that glacioclimatic conditions remained favourable to allow surge-cycle dynamics. Meteorological data show that since the 1970s, a warming trend has been causing glacier recession across the Tien Shan (Sorg et al., 2012). Records from Tien Shan meteorological station suggest that the warming may have been accompanied by reduced annual precipitation in the central Tien Shan (Khromova et al., 2003; Kutuzov and Shahgedanova, 2009). Climatic variations above ~4000 m asl are poorly known because of a scarcity of long-term meteorological monitoring at high elevations, so the precise climatic factors behind the mass balance of the Inylchek glaciers are uncertain. Aizen et al. (1997) extrapolated weather measurements at Tien Shan meteorological station to an elevation of ≈ 4476 m asl to derive an annual mass-balance index for the Inylchek Glaciers for 1940 to 1990. They inferred several phases of minor/moderate positive balance (in mid-1950s, early and late 1960s, around 1980) lasting up to a few years amidst longer periods of negative balance; their reconstructed cumulative mass balance exhibits a negative trend that deepens especially since the early 1970s, implying shrinkage of Northern Inylchek Glacier in the several decades before the surge. However, according to theoretical models of surging (section 1.1), a surge remains possible as long as the mass-balance distribution during the quiescent phase can cause sufficient thickening of the glacier's upper reservoir area to raise the driving stress to initiate fast sliding. For Northern Inylchek Glacier, the nonlinear distribution of increasing annual precipitation with elevation (Aizen and Aizen, 1997; Aizen et al., 1997) might have promoted such thickening. Unfortunately, remote sensing data of the upper glacier/trunk are not available for us to assess how the glacier surface topography there evolved before the surge. The elevation-differencing analysis of Shangguan et al. (2015) captured some topographic changes caused by the 1996 surge (see their Figs. 4a and 5), but, given the long interval

being studied, their analysis cannot resolve any local thickening of the upper glacier before surge initiation; such signal (if thickening did occur) is apparently masked by the surge signal. For understanding the glaciological processes underlying the surge, it would be valuable to conduct the elevation differencing for multiple short periods up until September 1996.

6.3. Refining the history of surge termination

The precise motion of the snout during the declining surge phase between 8 November, 1996 (stage I) and 6 June, 1997 (stage J) is not resolved by our imagery. Earlier we suggested that it reached the June 1997 position before that date. Knowledge of this part of the history can inform future efforts to model the surge dynamics. Here we use the recorded 5 December, 1996 jökulhlaup, together with assumptions, to further constrain the snout's evolution through stages H, I and J (Fig. 8).

First, note that the snout advance is unlikely to have experienced a sudden step-reduction in velocity on 8 November, as would happen if it faithfully followed the mean velocity estimate of 50 m d^{-1} for interval H to I, and 9 m d^{-1} for interval I to J (section 4.2). This is because there were no apparent obstacles midway across the Upper Lake (or its bed topography) against the advance (Fig. 6, I); any deceleration then was likely to be gradual. Furthermore, if we assume that continued filling of Lower Lake Merzbacher is necessary to trigger or hasten its outburst, then one can infer from the jökulhlaup date that the snout was still advancing across the Upper Lake to displace water into the Lower Lake on 3 December, 1996 (if we allow two days for flood-peak propagation to Xiehela), or at least until late November, if we account for extra time it takes for the flood discharge to rise to its peak (section 4.2.1).

These considerations lead us to posit three approximate scenarios for the snout motion, as follows. In scenario 1, after stage I, the snout continued to advance at 50 m d^{-1}

until it reached its near-maximal (June 1997) position, i.e., covering 1850 m in 37 days, to reach there on December 15, 1996 - well before June 1997. The surge duration (since stage G) in this scenario is 95 days. In 1997 summer, the snout then advanced by another ~100 m due to a mini-surge or speed-up event (section 4.4).

Scenario 2 envisages that after stage I, the snout again continued to advance at 50 m d^{-1} , but this fast surge phase ended ≈ 25 days later on around 3 December - if we assume the jökulhlaup was triggered then. On that day, the snout would have reached position X (Fig. 8), 1250 m downvalley of the position at stage I. It then advanced much more slowly afterwards, covering the remaining 600 m to the June 1997 position at a mean rate of 3.5 m d^{-1} . The total (fast-) surge duration is 82 days. This scenario is attractive because X lies just beyond where the Upper-Lake bed begins to slope upward (section 5) and the retrograde slope can be expected to slow the surge. This self-consistency within scenario 2 is not overly sensitive to the presumed date of flood initiation; it improves if we assume an earlier flood initiation in late November.

Finally, scenario 3 supposes a shortest possible surge: After stage I (8 November, 1996), the snout had advanced so quickly that it managed to reach the June-1997 position on the day of flood initiation (3 December, 1996); the surge then terminated. As in scenario 2, the surge duration is 82 days (or shorter if we assume earlier flood initiation). Scenario 3 requires the snout advance to have accelerated from interval H–I into the next interval between stage I and 3 December, with a mean rate of $\approx 74 \text{ m d}^{-1}$ during the latter interval.

All three scenarios invoke water displacement down the lake cascade to induce the flood; none of them upsets our conclusion of an Alaskan-type surge. Crucially, they all point to an active surge phase not exceeding ≈ 3 months - which is again consistent with an Alaskan-type surge. Our inference of a short surge duration here is fundamentally constrained by the high advance rate from stage H to I (50 m d^{-1}) and the limited distance

for the snout to cover after stage I (1850 m). With our present observational data, we cannot establish which scenario most closely resembles the actual history. Scenario 3 may seem less likely compared to scenarios 1 and 2 as it requires the snout to accelerate, but this is possible if water-saturated sediments on the lake bed lubricated basal sliding of the glacier farther.

Although the preceding arguments do not hinge on the (displaced/flood) volumes discussed in section 4.2.1, where we argued that the surge hastened the outburst, an intricacy of our assumption deserves comment. We are inferring here that the snout had to be moving forward (to displace water) when the flood initiated. This strictly requires two assumptions to be met: (i) a continued rise in the Lower Lake water level is necessary to initiate a flood; (ii) the rise was caused by the surge-displaced water input rather than (or as well as) other water sources entering the cascade. Assumption (ii) is supported probabilistically because any meltwater input is shown to be negligible compared to the displacement flux (section 4.2.1); i.e. we consider it unlikely that the snout was not advancing at flood initiation and the outburst was triggered by slow filling by meltwater only.

Assumption (i) concerns the physical mechanism of flood initiation. It is supported by theoretical modelling showing that continued lake-filling is required to overcome the hydraulic seal of an ice dam (Fowler 1999; Kingslake and Ng, 2013b). It also finds support in a meteorologically forced reconstruction of the long-term lake level history of Lower Lake Merzbacher (Ng and Liu, 2009), which shows that lake-level rise preceded most of the past jökulhlaups from this lake.

6.4. Role of glacier-lake interactions in the long-term cascade dynamics

Northern Inylchek Glacier interacted with its proglacial lake through most of our study period. This relationship may affect its surge-cycle dynamics in two ways. First, snout

retreat during the quiescent phase was probably enhanced by calving and melting at the ice-water contact. These ablation processes are known to depend on factors including lake-basin geometry (via changing water depth at the ice front) and lake thermal balance (which responds to meteorological factors and meltwater discharge from the glacier) - as has been recognized in studies of proglacial lake expansion (e.g., Sakai et al., 2009). These processes presumably operate during the surge as well, when they interact with trunk motion to determine how the snout position evolves. Calving was evidently rigorous during the surge, as shown by abundant icebergs on the Upper Lake through stages G to J (Figs. 6 and 7). Accurate modelling of surge-cycle dynamics of Northern Inylchek Glacier will need to account for these processes as well as the impact of extensive debris cover on the trunk on surface ablation rates. The coupling between snout position and proglacial-lake processes may also influence the glacier's longitudinal surface profile, and consequently its flow.

Second, the 1996 surge must have overridden thick sequences of former lake deposits that were probably unconsolidated and fine-grained; these properties could have enhanced soft-bed basal sliding (in ways different to subglacial sediments) and controlled the surge characteristics, including the spatiotemporal evolution of trunk-flow velocity and snout-advance distance. Thus, in terms of basal mechanics, the 1996 surge may share similarities with the surge of marine tidewater glaciers (e.g., Bering Glacier in Alaska; Post and Mayo, 1971). Our knowledge of the area reglaciated by the 1996 surge suggests that the sediment stratigraphy there consists of at least three horizons: (i) an upper layer of recent lake deposits accumulated during the expansion of the Upper Lake and retreat of Northern Inylchek Glacier between the 1940s and 1990s (section 4.1), which include formerly englacial and supraglacial sediments from the downwasting glacier; (ii) an intermediate layer of subglacial till associated with the glacial extent of the 1930s and early 1940s (Fig. 5A); and (iii) deeper underlying layers composed of older lake/till

deposits (Häusler et al., 2014). Further field studies are needed to unravel the glacial history of the area. Two avenues are to date the stable moraine-pond complex (including the arcuate moraines) to help disentangle its formation history and to extract sediment cores from both the Upper Lake and Lower Lake basins and interpret these cores for past fluctuations of both glaciers reaching back to before our study period.

Much of our analysis has focussed on the surge displacement of water from the Upper Lake in 1996. An important insight from this event is that fluctuations in the dynamics and meltwater output of Northern Inylchek Glacier can cause time-varying hydrological forcings on the lake cascade and the Lower Lake level, potentially affecting its outburst pattern. We suggested that a speedup/mini-surge of the glacier in summer 1997 might have helped trigger the July 1997 outburst (section 4.4). More generally, one could ask whether other floods from Lower Merzbacher Lake were induced/influenced by surging. According to the recorded flood dates (Liu, 1992; Ng and Liu, 2009; Glazirin, 2010), besides 1996, three other years (1958, 1966, 1988) had a late (November/December) flood, and some years had two floods (1956, 1957, 1960, 1966, 1980, and 1981). Because our imagery collection shows that Northern Inylchek Glacier retreated at a roughly steady rate between 1943 and 1996 (Fig. 8) and this period brackets all of the years listed above, it is unlikely that any of the late/second floods had been affected by surging. But we cannot rule out the possibility of minor/short-term snout advances not resolved by our images, which could have displaced water to help trigger a flood or bring forward its date.

Another interesting question is how much the glacier's retreat and attendant expansion of the Upper Lake from 1943 to 1996 constitute negative forcing on the water discharge at the outlet of the Upper Lake, in the sense that water is withheld by the lake. Over the 53 years, the volume withheld is $\approx 3700 \text{ m} \times 100 \text{ m}$ (lake depth) $\times 1000 \text{ m}$ (lake basin width) $\times 67\%$ (assuming parabolic-shaped bathymetric crosssection) $\approx 2.5 \times 10^8 \text{ m}^3$,

which implies a mean discharge reduction of $0.15 \text{ m}^3 \text{ s}^{-1}$. Although this value is much smaller than the flux through the Upper Lake sourced from glacial melt (section 4.2.1), it may have had a cumulative effect on the outburst timings of Lower Lake Merzbacher over decadal timescales.

7. Conclusions

We have analyzed the 1996 surge of Northern Inylchek Glacier in detail, concluding that it was an Alaskan-type surge with mean flow velocities on the glacier trunk reaching as much as 50 m d^{-1} (for the 32-day interval H to I; section 4.2) and a main surge phase lasting no longer than 3 months. The surge advanced the snout by 3.7 km. Observations derived for its evolution (including different scenarios for surge termination; section 6.3) provide vital data for constraining modelling simulations of the surge. To inform such modelling further, geophysical measurements are urgently needed to determine the thickness and bed topography of the glacier and preferably also its thermal regime.

Research should monitor the surface profile, flow speed, and mass balance of Northern Inylchek Glacier to understand whether/when it will evolve toward another surge and whether its response to regional warming will delay or prevent surging. Along with such effort, which will likely require glacier-flow modelling, it will be interesting to address what causes the dynamical contrast between Northern Inylchek Glacier and Southern Inylchek Glacier. Our study has successfully employed remote sensing data to reconstruct the surge sequence and surge cycle of Northern Inylchek Glacier. Other surging glaciers in the Tien Shan await study to a similar extent by this approach.

The Inylchek system, with a surging glacier lying upvalley of a cascade of two lakes - the Upper Lake being in contact with the surging glacier, and the Lower Lake being a source of repeated jökulhlaups as it is dammed by another glacier - presents an extreme example of the coupled interactions between glacier hydrology and glacier flow. Much

remains unknown about the system's history before the mid-nineteenth century and the hydrological characteristics and processes of both glaciers. It is hoped that our study will help promote a comprehensive understanding of the coupling.

Acknowledgements

Thanks to B. Moldobekov and his crew (at the Central Asian Institute of Applied Geosciences) and H. Echtler, J. Lauterjung, and H.-U. Wetzel (GeoForschungsZentrum Potsdam) for logistical support during our expeditions, and to V. A. Kuzmichenok and S. A. Erochin who kindly provided aerial photographs. The study benefited from valuable comments by J. Kargel, communications with G. Glazirin and B. Mavlyudov, and the constructive and thorough reviews by W. Häberli and two anonymous reviewers. This research is part of an FP7 ERA-NET CIRCLE project and we gratefully acknowledge funding by the Austrian Federal Ministry of Science and Research (grant no. BMWF-37.590/0001-II/4/201; principal investigators H. Häusler and D. Leber).

References

- Aizen, V.B, Aizen, E.M., 1997. Hydrological cycles on the North and South peripheries of mountain-glacial basins of Central Asia. *Hydrol. Processes*, 11, 451–469 (doi: 10.1002/(SICI)1099-1085(199704)11:5<451::AID-HYP448>3.0.CO;2-M).
- Aizen, V.B., Aizen, E.M., Dozier, J., Melack, J.M., Sexton, D.D., Nesterov, V.N., 1997. Glacial regime of the highest Tien Shan mountain, Pobeda-Khan Tengry massif. *J. Glaciol.*, 43(145), 503–512.
- Atlas of the Kyrgyz Republic, 1987. (in Russian), Moscow.

- Barrand, N.E., Murray, T., 2006. Multivariate controls on the incidence of glacier surging in the Karakoram Himalaya. *Arct. Antarct. Alp. Res.*, 38, 489–498.
- Benn, D.I., Evans, D.J.A., 2010. *Glaciers & Glaciation*. Hodder Education, London.
- Björnsson, H., Pálsson, F., Sigurðsson, O., Flowers, G.E., 2003. Surges of glaciers in Iceland. *Ann. Glaciol.*, 36, 82-90.
- Blagowischinski, B.P., Glazirin, G.E, Kokarev, A.L., Popov, D.I, Pimankina, N.B., Uwarov, B.I., 1998. To the heart of the Tien Shan (in Russian). 51 p., Institute of Geography, Scientific Academic Ministry, Academy of Sciences, Almati/ Kazach Republic.
- Bogen, J., Xu, M., Kennie, P., 2015. The impact of pro-glacial lakes on downstream sediment delivery in Norway. *Earth Surf. Process. Landforms*, 40, 942-952.
- Clarke, G.K.C., 1987. Fast glacier flow; ice streams, surging, and tidewater glaciers. *J. Geophys. Res.*, 92, B9, 8835-8841 (doi:10.1029/JB092iB09p08835).
- Copland, L., Sharp, M.J., Dowdeswell, J.A., 2003. The distribution and flow characteristics of surge-type glaciers in the Canadian High Arctic. *Ann. Glaciol.*, 36, 73–81 (doi:10.3189/172756403781816301).
- Cuffey, K.M., Paterson, W.S.B., 2010. *The Physics of Glaciers*. Elsevier, Amsterdam.
- Deutscher Alpenverein (Ed.), 2011. *Alpenvereinskarte 0/15 Khan Tengri, Tien Shan/Kyrgyzstan Trekking 1:100.000*. München.
- Evans, S.G., Tutubalina, O.V., Drobyshev, V.N., Chernomomoretz, S.S., McDougall, S., Petrakov, D.A., Hungr, O., 2009. Catastrophic detachments and high-velocity long-runout flow of Kolka Glacier, Caucasus Mountains, Russia. *Geomorphology*, 105, 314-321 (doi:10.1016/j.geomorph.2008.10.008).
- Farinotti, D., Huss, M., Bauder, A., Funk, M., Truffer, M., 2009. A method to estimate the ice volume and ice-thickness distribution of alpine glaciers. *J. Glaciol.*, 55(191), 422-430 (doi: /10.3189/002214309788816759).

- Fowler, A.C., 1999. Breaking the seal at Grímsvötn. *J. Glaciol.*, 45(151), 506–516.
- Fowler, A.C., Murray, T., Ng, F., 2001. Thermally controlled glacier surging. *J. Glaciol.*, 47 (159), 527–538 (doi:10.3189/172756501781831792).
- Frappé, T.P., Clarke, G.K.C., 2007. Slow surge of Trapridge Glacier, Yukon Territory, Canada. *J. Geophys. Res.*, 112, F03S32, 17 p. (doi:10.1029/2006JF000607).
- Gardner, J. S., 1990. A surge of Bualtar Glacier, Karakoram Range, Pakistan: a possible landslide trigger. *J. Glaciol.*, 36(123), 159-162.
- Glazirin, G.E., 2010. A century of investigations on outburst of the ice-dammed Lake Merzbacher (Central Tien Shan). *Austrian J. Earth Sci.*, 103(2), 171–179.
- Glazirin, G.E., Popov, V.I., 1999. North Inyl'chek Glacier during the last one and a half century (in Russian with English summary). *Data Glac. Stud.*, 87, 165–168.
- Harrison, W.D., Post, A.S., 2003. How much do we really know about glacier surging? *Ann. Glaciol.*, 36, 1-6 (doi:10.3189/172756403781816185).
- Harrison, W.D., Osipova, G.B., Nosenko, G.A., Espizua, L., Käab, A., Fischer, L., Huggel, C., Burns, P.A.C, Truffer, M., Lai, A.W., 2014. Glacier surges. In: Haeberli, W., Whiteman, C. (Eds.): *Snow and Ice-Related Hazards, Risks, and Disasters*, 437- 485 (doi: 10.1016/B978-0-12-394849-6.00013-5).
- Häusler, H., Leber, D., Scheibz, J., Kopecny, A., Wetzler, H.-U., Echtler, H., Moldobekov, B., 2010. Results from the 2009 Investigations at the Global Change Observatory "Gottfried Merzbacher" (Tien Shan, Kyrgyz Republic). *Geophys. Res. Abstr.*, 12, EGU2010-3660.
- Häusler, H., Scheibz, J., Leber, D., Kopecny, A., Echtler, H., Wetzler, H.-U., Moldobekov, B., 2011. Results from the 2009 expedition to the Inylchek Glacier, Central Tien Shan (Kyrgyzstan). *Austrian J. Earth Sci.*, 104/2, 47–57.

- Häusler, H., Kopecny, A., Leber, D., 2012a. Are the staircase terraces in the Inylchek Valley (Central Tien Shan, Kyrgyzstan) of neotectonic or sedimentary origin? *Geophys. Res. Abstr.*, 14, EGU2012-5278-1.
- Häusler, H., Kopecny, A., Leber, D., 2012b. Recent fluctuations of the Northern Inylchek Glacier (Central Tien Shan, Kyrgyzstan). In: Severskiy, I.V. (Ed.): *Cryosphere of Eurasian Mountains. Abstracts of the International Conference devoted to the opening of the Central Asian Regional Glaciological Centre as a Category 2 Centre under the auspices of UNESCO*, Institute of Geography, Almaty/Kazachstan, pp. 9-10.
- Häusler, H., Leber, D., Kopecny, A., 2012c. Is Upper Lake Merzbacher (Central Tien Shan, Kyrgyzstan) the result of a fluctuating glacier? *Geophys. Res. Abstr.*, 14, EGU2012-5327.
- Häusler, H., Kopecny, A., Leber, D., Wagreich, M., Gier, S., Hruby-Nichtenberger, S., 2014. Sedimentology of Paleolake Merzbacher in the Northern Inylchek Valley (Central Tien Shan, Kyrgyzstan). *Austrian J. Earth Sci.*, 107(2), 74–88.
- Hewitt, K., 2014. *Glaciers of the Karakoram Himalaya: Glacial Environments, Processes, Hazards and Resources*. Springer, Dordrecht.
- Jiskoot, H., 2011. Glacier surging. In: Singh, V.P., Sing, P., Haritashya, U.K. (Eds.): *Encyclopedia of snow and glaciers*. Springer, Dordrecht, pp. 415–428.
- Jiskoot, H., Murray, T., Boyle, P., 2000. Controls on the distribution of surge-type glaciers in Svalbard. *J. Glaciol.*, 46 (154), 412–422
(doi:10.3189/172756500781833115).
- Kamb, B., Raymond, C.F., Harrison, W.D., Engelhardt, H., Echelmeyer, K.A., Humphrey, N., Brugman, M.M., Pfeffer, T., 1985. Glacier surge mechanism: 1982-1983 surge of Variegated Glacier, Alaska. *Sci., New Ser.*, 227(4686), 469–479.

- Kargel, J.S., Abrams, M.J., Bishop, M.P., Bush, A., Hamilton, G., Jiskoot, H., Käab, A., Kieffer, H.H., Lee, E.M., Paul, F., Rau, F., Raup, B., Shroder, J.F., Soltesz, D., Stainforth, D., Stearns, L., Wessels, R., 2005. Multispectral imaging contributions to global land ice measurements from space. *Remote Sens. Environ.*, 99, 187–219 (doi:10.1016/j.rse.2005.07.004).
- Kennie, P.D., 2012. Sedimentation patterns in a Norwegian glacial lake with focus on climate-related hydrological processes. Master Thesis, Univ. Life Sciences, Ås, Norway.
- Khromova, T.E., Dyurgerov, M.B., Barry, R.G., 2003. Late-twentieth century changes in glacier extent in the Ak-shirak Range, Central Asia, determined from historical data and ASTER imagery. *Geophys. Res. Lett.*, 30(16), 1863 (doi:10.1029/2003GL017233).
- Kingslake, J., Ng, F., 2013a. Quantifying the predictability of the timing of jökulhlaups from Merzbacher Lake, Kyrgyzstan. *J. Glaciol.*, 59(217), 805–818 (doi:10.3189/2013JoG12J156).
- Kingslake, J., Ng, F., 2013b. Modelling the coupling of flood discharge with glacial flow during jökulhlaups. *Ann. Glaciol.*, 54(63), 25–31 (doi:10.3189/2013AoG63A331).
- Konovalov, V.G., 1990. Method of calculation and forecast of regime elements of the dangerous Merzbacher Lake (in Russian with English summary). *Data Glac. Stud.*, 69, 141-147.
- Kopečný, A., 2014. Geologische und glazialgeomorphologische Untersuchungen im Bereich des Inylchek Gletschers (Tien Shan, Republik Kirgistan)(in German). Master Thesis, Univ. Vienna, Austria.
- Kotlyakov, V.M., Osipova G.V., Tsvetkov, D.G., 2008. Monitoring surging glaciers of the Pamirs, Central Asia from space. *Ann. Glaciol.*, 48, 125–133 (doi:10.3189/172756408784700608).

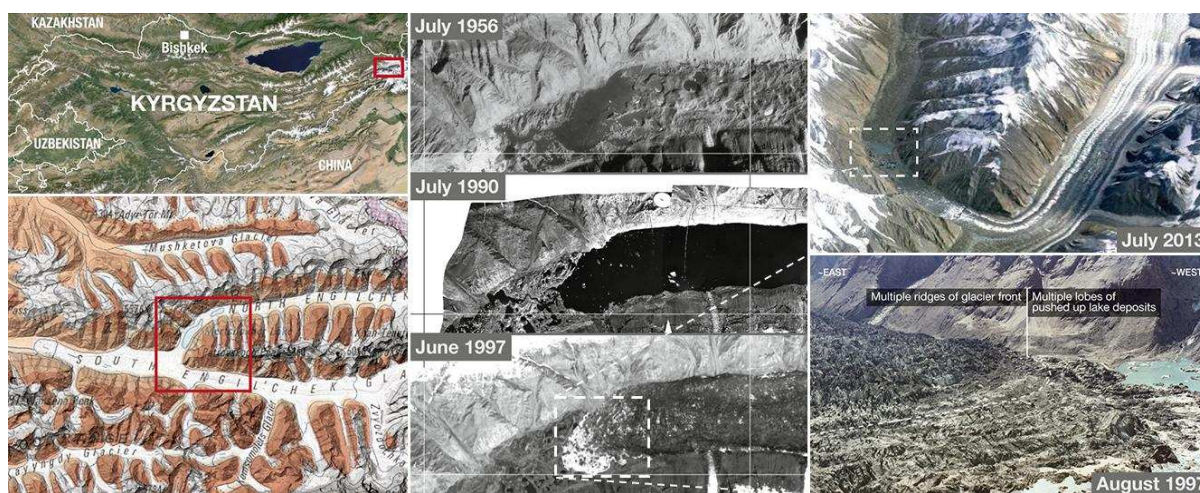
- Kotlyakov, V.M., Dyakova, A.M., Koryakin, V.S., Kravtsova, V.I., Osipova, G.B., Varnakova, G.M., Vinogradov, V.N., Vinogradov, O.N., Zverkova, N.M., 2010. Glaciers of the former Soviet Union. In: Williams, R.S., Ferrigno, J.G. (Eds.), Satellite image atlas of glaciers of the world: ASIA. U.S. Geol. Surv. Prof. Paper, 1386-F-1, III-VIII, F1-F125, Washington.
- Krysanova, V., Wortmann, M., Bolch, T., Merz, B., Duethmann, D., Walter, J., Huang, S., Tong, J., Buda, S., Kundzewicz, Z.W., 2015. Analysis of current trends in climate parameters, river discharge and glaciers in the Aksu River basin (Central Asia). *Hydrological Sciences Journal*, 60(4), 566-590 (doi: 10.1080/02626667.2014.925559).
- Kutuzov, S., Shahgedanova, M., 2009. Glacier retreat and climatic variability in the eastern Terskey-Alatau, inner Tien Shan between the middle of the 19th century and the beginning of the 21st century. *Glob. Planet. Change*, 69, 59–70 (doi:10.1016/j.gloplacha.2009.07.001).
- Kuzmichenok, V.A., 1983. Stereophotogrametric size determination technology of occasionally disgorging glacial lakes (by the example of Merzbaher Lake). Information sheet about scientific and technical achievement No. 32-83. Kyrgyz Republican Institute of Science-technical Information and Advocacy of State Planning Committee of the Kyrgyz Soviet Socialist Republic (in Russian).
- Leber, D., Kopecny, A., Häusler, H., Wetzler, H.-U., 2009. Ground check for remote sensing based monitoring of the central Inylchek glacier system (Kyrgyz Republic). Glacier hazard workshop 2009, Vienna, Poster session, BOKU Univ., Vienna, Austria
(https://www.baunat.boku.ac.at/fileadmin/data/H03000/H87000/H87200/4Veranstaltungen/6.8_Leber.pdf).

- Li, H., Ng, F., Li, Z., Qin, D., Cheng, G., 2012. An extended ‘perfect-plasticity’ method for estimating ice thickness along the flow line of mountain glaciers. *J. Geophys. Res.*, 117, F01020 (doi:10.1029/2011JF002104).
- Li, J., Li, Z., Zhu, J., Ding, X., Wang, Ch., Chen, J., 2013. Deriving surface motion of mountain glaciers in the Tuomuer-Khan Tengri mountain ranges from PALSAR images. *Glob. Planet. Change*, 101, 61–71 (doi:10.1016/j.gloplacha.2012.12.004).
- Liu, J., 1992. Jökulhlaups in the Kunmalike River, southern Tien Shan mountains, China. *Ann. Glaciol.*, 16, 85–88.
- Macheret, Yu.Ya., Nikitin, S.A., Babenko, A.N., Vesnin, A.V., Bobrova, L.I., Sankina, L.V., 1993. Thickness and structure of the Southern Inylchek Glacier from the data of radio echo sounding (in Russian with English summary). *Data Glac. Stud.*, 77, 86–97.
- Mavlyudov, B.R., 1995. Tongue oscillations of Northern Inylchek Glacier (in Russian with English summary). *Data Glac. Stud.*, 79, 95–98.
- Mavlyudov, B.R., 1997. Drainage of the ice-dammed Merzbacher Lake, Tien Shan (in English). *Data Glac. Stud.*, 81, 61–65.
- Mavlyudov, B.R., 1998. Expedition to the Inylchek Glacier (in Russian). *Data Glac. Stud.*, 84, p. 24.
- Mayer, C., Fowler, A.C., Lambrecht, A., Scharrer, K., 2011. A surge of North Gasherbrum Glacier, Karakoram, China. *J. Glaciol.*, 57(204), 904–916 (doi:10.3189/002214311798043834).
- Meier, M.F., Post, A.S., 1969. What are glacier surges? *Can. J. Earth Sci.*, 6, 807–817.
- Meiners, S., 1997. Historical to Post Glacial glaciation and their differentiation from the Late Glacial period on examples of the Tian Shan and the N.W. Karakorum. *Geojournal*, 42, 259–302.

- Merzbacher, G., 1905. The Central Tian-Shan Mountains (1902-1903). 294 p., 1 map 1:1.000.000, J. Murray Publ., London.
- Merzbacher, G., 1906. Der Tian-Schan oder das Himmelsgebirge. Skizze von einer in den Jahren 1902 und 1903 ausgeführten Forschungsreise in den zentralen Tian Schan (in German). Z. Dtsch. Österr. Alpenver., 37, 121–151, München.
- Murray, T., Dowdeswell, J.A., Drewry, D.J., Frearson, I., 1998. Geometric evolution and ice dynamics during a surge of Bakaninbreen, Svalbard. J. Glaciol., 44(147), 263–272.
- Neelmeijer, J., Motagh, M., Wetzel, H.-U., 2014. Estimating spatial and temporal variability using TerraSAR-X data. Remote Sens., 6, 9239–9259 (doi:10.3390/rs6109239).
- Ng, F., Liu, S., 2009. Temporal dynamics of a jökulhlaup system. J. Glaciol., 55(192), 651–665 (doi:10.3189/002214309789470897).
- Ng, F., Liu, S., Mavlyudov, B., Wang, Y., 2007. Climatic control on the peak discharge of glacier outburst floods. Geophys. Res. Lett., 34, L21503 (doi:10.1029/2007GL031426).
- Nobakht, M., Motagh, M., Wetzel, H.-U., Roessner, S., 2011. Surface velocity field of the Inylchek Glacier/Kyrgyzstan – studied with LANDSAT data imagery. DGPF-Tagungsband, 20, 289–294, (Deutsche Gesellschaft für Photogrammetrie, Fernerkundung und Geoinformation), Potsdam.
- Osipova, G.B., Tsetkov, D.G., Rudak, M.S., 1998. Inventory of the Pamirs surging glaciers (in Russian). Data Glac. Stud., 85, 3–136.
- Osmonov, A., Bolch, T., Xi, C., Kurban, A., Guo, W., 2013. Glacier characteristics and changes in the Sary-Jaz River Basin (Central Tien Shan, Kyrgyzstan) 1990-2010. Remote Sens. Lett., 4, 725–734 (doi:10.1080/2150704X.2013.789146).

- Philip, G., Sah, M.P., 2004. Mapping repeated surges and retreat of glaciers using IRS-1C/1D data: a case study of Shaune Garang glacier, northwestern Himalaya. *Int. J. Appl. Land Obs. Geoinform.*, 6, 127–141.
- Pieczonka, T., Bolch, T., 2015. Region-wide glacier mass budgets and area changes for the Central Tien Shan between ~ 1975 and 1999 using Hexagon KH-9 imagery. *Glob. Planet. Change*, 128, 1-13 (doi:10.1016/j.gloplacha.2014.11.014).
- Pieczonka, T., Bolch, T., Junfeng, W., Shiyin, L., 2013. Heterogenous mass loss of glaciers in the Aksu-Tarim Catchment (Central Tien Shan) revealed by 1976 KH-9 Hexagon and 2009 SPOT-5 stereo imagery. *Remote Sens. Environ.*, 130, 233–244 (doi:10.1016/j.rse/2012.11.020).
- Post, A., Mayo, L.R., 1971. Glacier dammed lakes and outburst floods in Alaska. *Hydrologic Investigations, Atlas HA-455*, U.S. Geological Survey, Washington.
- Quincey, D.J., Braun, M., Glaser, N.F., Bishop, M.P., Hewitt, K., Luckman, A., 2011. Karakoram glacier surge dynamics. *Geophys. Res. Lett.*, 38, L18504 (doi:10.1029/2011GL049004,2011).
- Raymond, C.F., 1987. How do glaciers surge? A review. *J. Geophys. Res.*, 92 (B9), 9121–9134 (doi:10.1029/JB092iB09p09121).
- Sakai, A., Nishimura, K., Kadota, T., Takeuchi, N., 2009. Onset of calving at supraglacial lakes on debris-covered glaciers of the Nepal Himalaya. *J. Glaciol.* 55(193), 909-917 (doi:10.3189/002214309790152555).
- Scheibz, J., Häusler, H., Leber, D., Kopečný, A., Wetzel, H.-U., 2009. Near surface geophysical measurements in the vicinity of Lake Merzbacher. First results from the 2009 Inylchek Expedition (Kyrgyz Republic). *Glacier Hazard Workshop 2009 Vienna, Poster Session, BOKU Univ., Vienna, Austria* (https://www.baunat.boku.ac.at/.../6.7_Haeusler.pdf).

- Schiefer, E., Gilbert, R., 2008. Proglacial sediment trapping in recently formed Silt Lake, Upper Lillooet Valley, Coast Mountains, British Columbia. *Earth Surf. Proc. Landf.*, 33, 1542–1556 (doi:10.1002/esp.1625).
- Shangguan, D.H., Bolch, T., Ding, Y.J., Kröhnert, M., Pieczonka, T., Wetzel, H.-U., Liu, S.Y., 2015. Mass changes of Southern and Northern Inylchek Glacier, Central Tian Shan, Kyrgyzstan, during ~ 1975 and 2007 derived from remote sensing data. *The Cryosphere*, 9, 703–717 (doi:10.5194/tc-9-703-2015).
- Solomina, O., Barry, R., Bodnya, M., 2004. The retreat of Tien Shan glaciers (Kyrgyzstan) since the Little Ice Age estimated from aerial photographs, lichenometric and historical data. *Geogr. Ann.*, 86A, 205–215.
- Sorg, A., Bolch, T., Stoffel, M., Solomina, O., Beniston, M., 2012. Climate change impacts on glaciers and runoff in Tien Shan (Central Asia). *Nature Climate Change*, 2, 725–731 (doi:1038/nclimate1592).
- Wortmann, M., Krysanova, V., Kundzewicz, Z.W., Su, B., Li, X., 2013. Assessing the influence of the Merzbacher Lake outburst floods on discharge using the hydrological model SWIM in the Aksu headwaters, Kyrgyzstan/NW China. *Hydrol. Process.*, 28(26), 6337–6350 (doi:10.1002/hyp.10118).
-



Graphical abstract

Highlights

- First detailed description of glacier surge in central Tien Shan, eastern Kyrgyzstan
 - Time series analysis of remote sensing images 1943-2011
 - Analysis of “chain reaction” linking water displacement by a surging glacier to triggering of a glacier lake outburst flood
 - Field investigations of the morphology of a surge-type glacier and bathymetry of its proglacial lake
-